IMMUNOLOGY

Immunopeptidome analysis reveals SERPINB3 as an autoantigen driving eczematized psoriasis

Manja Jargosch^{1,2}†, Jomy Kuruvila¹†, Emanuele Scala^{3,4}, Johannes Grosch², Jessica Eigemann^{1,2,5}, Sophia Wasserer^{1,2}, Shalva Lekiashvili¹, Nico Trautwein⁶, Daniel Johannes Kowalewski⁶, Alexander Böhner¹, Yigit Köseoglu^{1,2}, Christina Hillig^{7,8}, Jenny Thomas^{1,2,3}, Felix Lauffer^{1,2,5}, Carsten B. Schmidt-Weber^{2,9}, Michael P. Menden^{7,10}, Juliane S. Walz^{6,11,12,13,14}, Susanne Kaesler¹, Stefanie Eyerich², Simon Blank², Hans-Georg Rammensee^{6,12,14}, Tilo Biedermann¹, Kilian Eyerich^{3,4}, Zsuzsanna Kurgyis¹†, Lena K. Freudenmann^{6,12,14}†, Natalie Garzorz-Stark^{1,3,4}*†

Psoriasis (Pso) is a chronic inflammatory skin disease driven by T helper 17 (T_H17) cells, with several clinical subtypes. While self-reactive immune responses have been observed, the role of autoantigens in Pso remains unclear. Using immunopeptidomics, we identified serpin family B member 3 (SERPINB3) and SERPINB4 as candidate autoantigens in Pso skin. In a mouse model, the SERPINB3 ortholog Serpinb3b enhanced inflammation, promoted tissue-resident memory T cells, and skewed immunity toward a T_H2 phenotype. In humans, SERPINB3 reactivity was specifically associated with "eczematized psoriasis" (EczPso), a subtype marked by T_H2/T_H17 immune signatures. SERPINB3 protein was enriched in EczPso lesions and highly secreted by keratinocytes under combined T_H2/T_H17 stimulation. Lesional T cells from EczPso—but not from eczema or classical plaque Pso—proliferated in response to SERPINB3 and induced EczPso-like features in a skin model. Our findings identify SERPINB3 as an autoantigen driving a distinct Pso subtype, supporting more precise diagnosis and therapy.

Copyright © 2025 The
Authors, some rights
reserved; exclusive
licensee American
Association for the
Advancement of
Science. No claim to
original U.S.
Government Works.
Distributed under a
Creative Commons
Attribution
NonCommercial
License 4.0 (CC BY-NC).

INTRODUCTION

Psoriasis (Pso) is a common chronic, inflammatory skin disease affecting an estimated 2 to 3% of the world population (1). It is characterized by high genetic and phenotypic heterogeneity including classical plaque-type, inverse, eczematized, and pustular variants (2–4). Decades of research have helped to identify an exaggerated T helper 17 (T_H17) immune response as the key driver of Pso responsible also for the histological Pso hallmarks such as a thickened epidermal layer (acanthosis), elongated rete ridges, and infiltration of neutrophils (5). The central role of T_H17/type 3 cytokines in Pso has been proven by the efficacy of modern Pso therapies targeting key molecules of the T_H17 pathway (6–12). Genetic analyses identified *HLA-C* at the Psoriasis Susceptibility 1 (*PSORS1*) gene locus exhibiting a strong association with the development of Pso (13), and

¹Department of Dermatology and Allergy, Technical University of Munich, Munich, Germany. ²ZAUM—Center of Allergy and Environment, Technical University of Munich, School of Medicine and Health & Helmholtz Munich, German Research Center for Environmental Health, Munich, Germany. ³Division of Dermatology and Venereology, Department of Medicine Solna, and Center for Molecular Medicine, Karolinska Institutet, Stockholm, Sweden. ⁴Department of Dermatology and Venereology, Medical Center, Faculty of Medicine, University of Freiburg, Freiburg, Germany. ⁵Department of Dermatology and Allergy, LMU Hospital, Munich, Germany. ⁶Institute of Immunology, University of Tübingen, Tübingen, Germany. ⁷Department of Computational Health, Institute of Computational Biology, Helmholtz Munich, Neuherberg, Germany. 8 Department of Mathematics, Technical University of Munich, Munich, Germany. ⁹German Center of Lung Research (DZL), Neuherberg, Germany. ¹⁰Department of Biochemistry & Pharmacology, Bio21 Molecular Science and Biotechnology Institute, The University of Melbourne, Melbourne, Australia. 11 Department of Peptide-based Immunotherapy, Institute of Immunology, University and University Hospital Tübingen, Tübingen, Germany. ¹²Cluster of Excellence iFIT (EXC 2180) "Image-Guided and Functionally Instructed Tumor Therapies", University of Tübingen, Tübingen, Germany. ¹³Clinical Collaboration Unit Translational Immunology, Department of Internal Medicine, University Hospital Tübingen, Tübingen, Germany. 14German Cancer Consortium (DKTK) and German Cancer Research Center (DKFZ), partner site Tübingen, Tübingen, Germany.

*Corresponding author. Email: natalie.garzorz-stark@uniklinik-freiburg.de †These authors contributed equally to this work.

several human skin-derived autoantigens that are recognized by specific T cells including keratin 17 (KRT17), cathelicidin antimicrobial peptide (LL37), ADAMTS-like protein 5 (ADAMTSL5), desmoglein 3 (DSG3), phospholipase A2 group IVD (PLA2G4D), and the serpin family B member 3 (SERPINB3)/SERPINB4-derived peptide Pso p27 have been described and proposed as potential drivers of Pso (14–19). However, none of the described antigens have been assigned a role for the immune cascade underlying Pso development or for shaping a distinct clinical phenotype of Pso.

In this study, we used an unbiased immunopeptidome-guided approach, a method typically used to identify targets for cancer immunotherapy (20-23), to identify yet-undescribed autoantigens in the skin of the disease spectrum of Pso. Immunopeptidomics allows for direct identification of human leukocyte antigen (HLA) class I and II ligands present in patient tissue specimens. This study was set up to retrieve a broad spectrum of putative autoantigens from welldefined patients with Pso to be able to also correlate autoantigens, e.g., to individual patients with Pso and phenotypes. Using this technique, we identified HLA-presented peptides derived from the serine protease inhibitors SERPINB3 and SERPINB4 exclusively presented on HLA class I in Pso skin. SERPINB3 and SERPINB4 are very closely related homologs (98% nucleotide and 92% amino acid sequence identity) (24) that are expressed in thymic Hassall's corpuscles, skin, and airway epithelium, with roles in regulating of Ecadherin expression and cell migration (25).

In a murine model of Pso-like dermatitis, the cutaneous supplementation of the SERPINB3 murine ortholog Serpinb3b demonstrated enhanced inflammation and promoted tissue-resident memory T cells (TRMs), contributing to the persistence of inflammation. In addition, Serpinb3b shifted the immune response toward a $T_{\rm H2}$ profile in murine skin, aligning with our observation that, in humans, SERPINB3 reactivity was especially found in patients clinically presenting with the Pso subtype "eczematized psoriasis" (EczPso) characterized by a mixed $T_{\rm H2}$ /type 2 and $T_{\rm H17}$ /type 3 immune signature.

Thus, we identified putative autoantigens in Pso and assigned a role of SERPINB3 to deviating the immune cascade in Pso toward a mixed $T_{\rm H2}$ coexpressing signature characterizing the phenotype of the Pso subtype EczPso. We provide evidence that proteins such as SERPINB3 actively drive distinct clinical Pso subtypes by shaping the immune response toward a subtype characterizing immune signature also contributing to Pso chronification by tissue-resident T cells. Thus, establishing SERPINB3 as an autoantigen with a distinct functional role also provides a basis for more stratified diagnostics and a subtype-specific treatment in Pso.

RESULTS

Immunopeptidome analysis of the skin unveils SERPINB3 and SERPINB4 as candidate Pso autoantigens

Using an unbiased approach, immunopeptidome analysis was conducted to identify unreported putative autoantigens in Pso skin. HLA ligands were isolated by immunoaffinity purification from skin samples of patients with Pso (Pso, n = 17), healthy controls (H, n = 10), and healthy autopsy-derived skin (AUT-DN, n = 9) and subsequently analyzed by liquid chromatography coupled with tandem mass spectrometry (LC-MS/MS).

Because of the promiscuous peptide binding of HLA class II molecules (26–28), we focused on the HLA class I peptidome with a well-established binding prediction. Comparative analysis of Pso versus healthy and autopsy-derived skin (Fig. 1A) identified 618 source proteins unique to Pso skin (Fig. 1B), with 613 excluded for being detected in fewer than four samples (<18%), reflecting low relevance and confidence. Among the five Pso-exclusive hits—SERPINB3, SERPINB4, PITPNA, AHSG, and SERPIND1—that were detected in at least 4 of 17 patient samples (Fig. 1C), only SERPINB3- and SERPINB4-derived peptides were confidently identified as HLA class I binders based on their sequences.

In 7 of 17 patients with Pso (41%), SERPINB3 and SERPINB4 were the most enriched HLA class I-presented antigens (Fig. 1C), with two patients also showing HLA class II-derived peptides for SERPINB3 and SERPINB4. A total of 19 different HLA class I- and HLA class II-presented peptides for SERPINB3 (Fig. 1D and table S1) and SERPINB4 (Fig. 1E and table S1) were identified in Pso skin. Neither healthy skin nor autopsy-derived skin showed SERPINB3or SERPINB4-derived HLA peptides, with the exception of sample AUT-DN04, in which two HLA class II peptides were detected (Fig. 1, D and E). The sequences of 16 identified SERPINB3 and SERPINB4 peptides were validated by comparing fragment spectra of experimental and synthetic heavy isotope-labeled peptides (fig. S1). Previously reported Pso antigens were not detected (ADAMTSL5/Q6ZMM2), failed quality control (e.g., nonproteotypic, atypical length, or inconsistent sequences; KRT17-Q04695 and LL37-P49913), and/or were common in healthy skin (DSG3-P32926, KRT17-Q04695, and LL37-P49913). File S1 lists HLA class I and II peptides, with total peptide counts per samples shown in fig. S2. Incidentally, HLA typing of patient peripheral blood mononuclear cells (PBMCs; Histogenetics LLC, Ossining, USA) revealed no specific allotype including the Pso-associated HLA-Cw6 variant (file S2). Skin immunopeptidome analysis identified SERPINB3 and SERPINB4 as the most abundant autoantigens in Pso presented on both HLA class I and II molecules, independent of a specific HLA allotype.

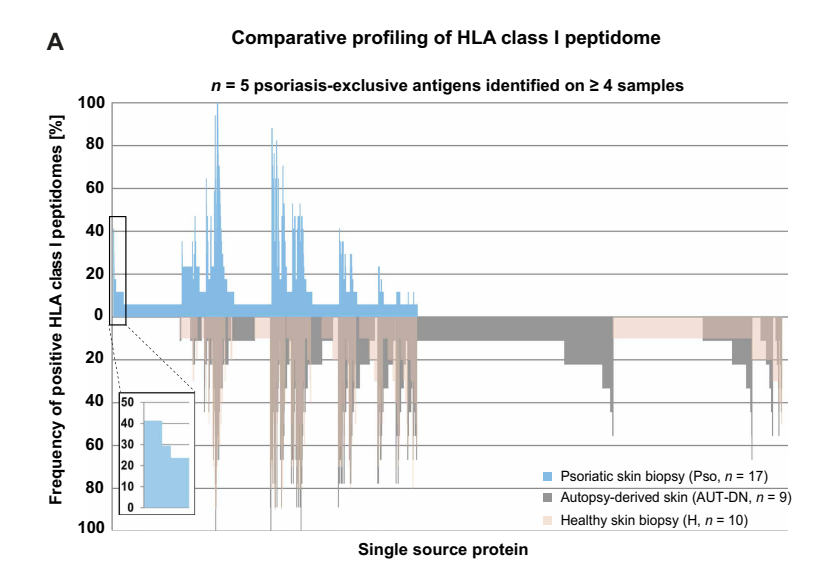
Serpinb3b augments skin inflammation and induces an immune deviation toward a mixed T_H1/T_H2 profile in vivo

We next sought to explore a role of SERPINB3 for Pso development in vivo. Wild-type mice (n=5 per group) were injected intradermally with 25 µg of native Serpinb3b (S), the murine homolog of SERPINB3, into one ear on days 0 and 3. As controls, we included nonfunctional heat-inactivated Serpinb3b (H) and mouse serum albumin (MSA, M). Our screening for immune consequences of cutaneous exposure to Serpinb3b included both a group of otherwise untreated mice with healthy skin and a group of mice treated with imiquimod (IMQ) for 6 days (days 0 to 5) to induce a well-established Pso-like dermatitis (29-31). Ear thickness was measured daily, and samples for histology, T cell infiltration, and cytokine analyses were harvested on day 6 (Fig. 2A).

Injection of native or heat-inactivated Serpinb3b alone already induced skin inflammation over time compared to the MSA control, as shown by ear swelling (Fig. 2, B and C). On day 6, ear thickness was significantly higher in the native (356 \pm 6.2 μ m, P < 0.0001) and heatinactivated (278.0 \pm 4.9 μ m, P = 0.0023) Serpinb3b groups compared to MSA (238 \pm 1.2 μ m). IMQ application further increased ear swelling in all groups (P < 0.0001). Notably, native Serpinb3b injection into skin additionally exposed to IMQ caused the largest increase of ear thickness (466 \pm 9.9 μ m), significantly higher than MSA (302 \pm 8.0 μ m, P < 0.0001) and heat-inactivated Serpinb3b (327 \pm 4.6 μ m, P < 0.0001) under IMQ (Fig. 2C), which was confirmed by histology (Fig. 2D). Both native and heat-inactivated Serpinb3b groups already showed immune cell infiltration, which was strongly enhanced by IMQ. Serpinb3b injection primarily caused immune cell infiltration, while IMQ also increased epidermal thickness (Fig. 2D). Flow cytometry analysis of ear-infiltrating immune cells confirmed significant T cell infiltration in both native Serpinb3b (28,668 \pm 3764 cells, P = 0.0055) and heatinactivated (26,570 \pm 5679 cells, P = 0.0037) Serpinb3b groups compared to MSA (12,008 ± 1787 cells) with IMQ further increasing infiltration (Fig. 2E).

Further characterization of cutaneous T cell infiltrates revealed that Serpinb3b injection increased the number of interleukin-17A (IL-17A)–producing (S: P=0.0219; H: P=0.0080), IL-4–producing (S: P=0.0682; H: P=0.0252), and IL-13–producing (S: P=0.0110; H: P=0.0009) CD3⁺ T as well as of T_H1 cytokine–expressing T cells [P=0.0104 (S) or P=0.0106 (H) for interferon- γ (IFN- γ); P=0.0810 (S) or P=0.0735 (H) for tumor necrosis factor (TNF)] (Fig. 2F). At the mRNA level, native and heat-inactivated Serpinb3b induced both T_H2/type 2 (Il13) and some T_H17/type 3 (Il22 and Il23) genes in the ear skin, while IMQ clearly increased T_H17/type 3 gene induction and promoted Serpinb3b-specific induction of Il6, Il62, Il63, Il64, Il6

To further study consequences of in vivo exposure to SERPINB3, ex vivo T cell proliferation assays were conducted. Immune cells from ear-draining lymph nodes were isolated on day 6, stained with carboxy-fluorescein succinimidyl ester (CFSE), and cocultured with Serpinb3b-pulsed bone marrow–derived dendritic cells (BMDCs) for 4 days. Relative frequencies of proliferating T cells compared to the control groups without Serpinb3b presentation were examined by flow cytometry. T cells from native (10.74 \pm 2.63%, P=0.0207) and heat-inactivated (11.04 \pm 1.47%, P=0.0024) Serpinb3b-injected mice showed significant proliferation upon Serpinb3b presentation by BMDCs, while T



409 460 ■ Psoriatic skin biopsy (Pso, *n* = 17) ■ Autopsy-derived skin (AUT-DN, *n* = 9) ■ Healthy skin biopsy (H, *n* = 10)

HLA class I-presented antigens

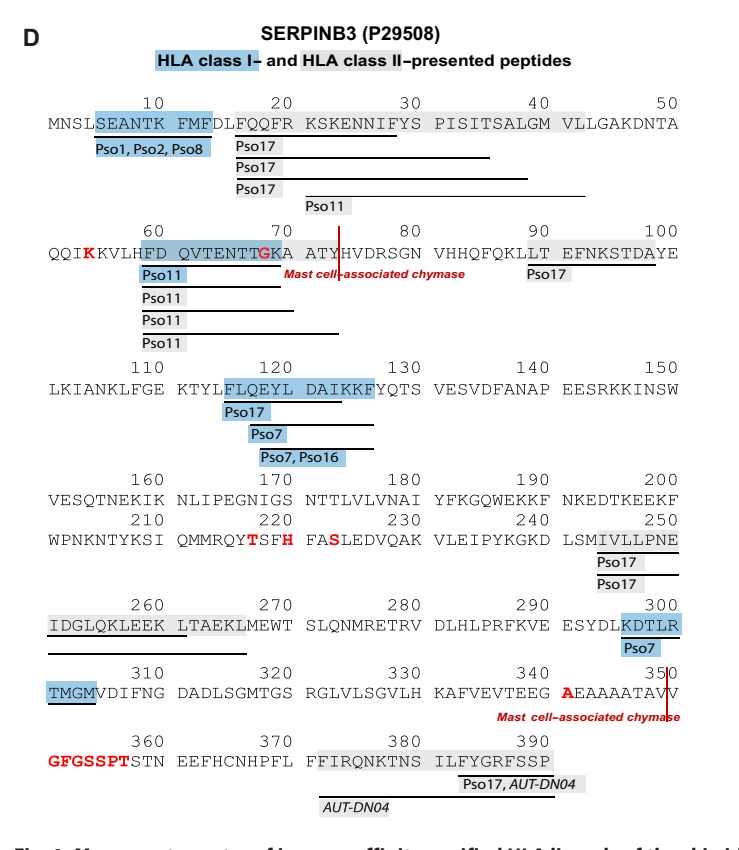
В

Ε

C Proteir Positive Pso biopsies symbol Accession Name SERPINB3 P29508 Serpin Family B Member 3 41.18% SERPINB4 P48594 Serpin Family B Member 4 41.18% *PITPNA Q00169 Phosphatidylinositol Transfer Protein Alpha 5 29.41% *AHSG P02765 Alpha 2-HS Glycoprotein 23 53% *SERPIND1 P05546 Serpin Family D Member 1 23.53%

SERPINB4 (P48594)

HLA class I- and HLA class II-presented peptides



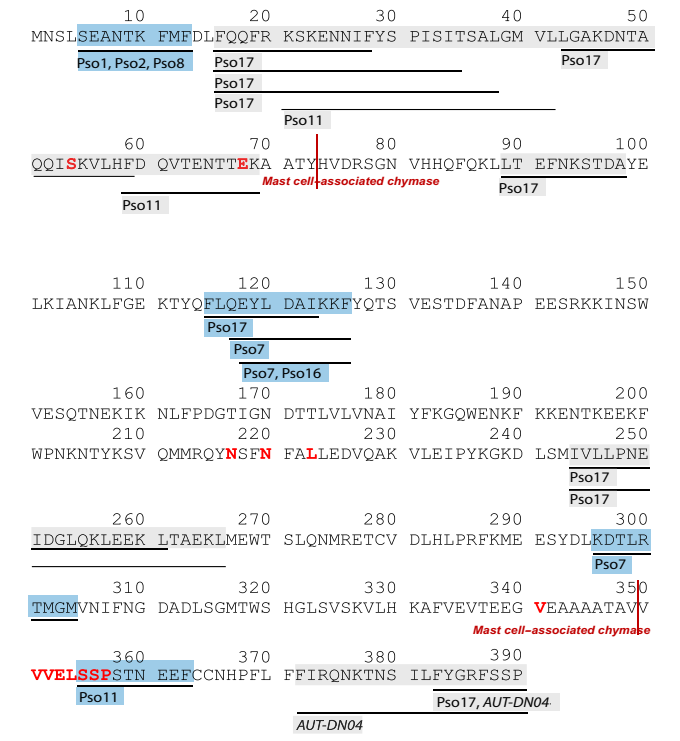


Fig. 1. Mass spectrometry of immunoaffinity-purified HLA ligands of the skin identified SERPINB3 and SERPINB4 as putative autoantigens in Pso. (A and B) Comparative profiling of the HLA class I peptidome of Pso skin (n = 17, Pso, blue) compared to healthy (n = 10, apricot) or healthy autopsy-derived skin (n = 9, AUT-DN, gray). Each bar in the waterfall plot (A) (associated with the x axis) represents a single source protein, whereas the frequency of positive HLA peptidomes is shown on the y axis. The Venn diagram (B) illustrates the number of distinct HLA class I-presented antigens per group. (C) Proteins exclusively identified in at least four psoriatic skin samples. (D and E) Annotation of HLA class I (indicated in blue)— and HLA class II (indicated in gray)—presented peptides to SERPINB3 (D) and SERPINB4 (E) protein sequences. Amino acids specific for either SERPINB3 or SERPINB4 are highlighted in red. Likewise, cleavage sites of the mast cell-associated chymase (18) are indicated in dark red. HLA, human leukocyte antigen; Pso, psoriasis; AUT-DN, autopsy-derived skin; H, healthy.

^{*} insufficient confidence of corresponding peptide identifications due to lack of HLA class I binding motifs

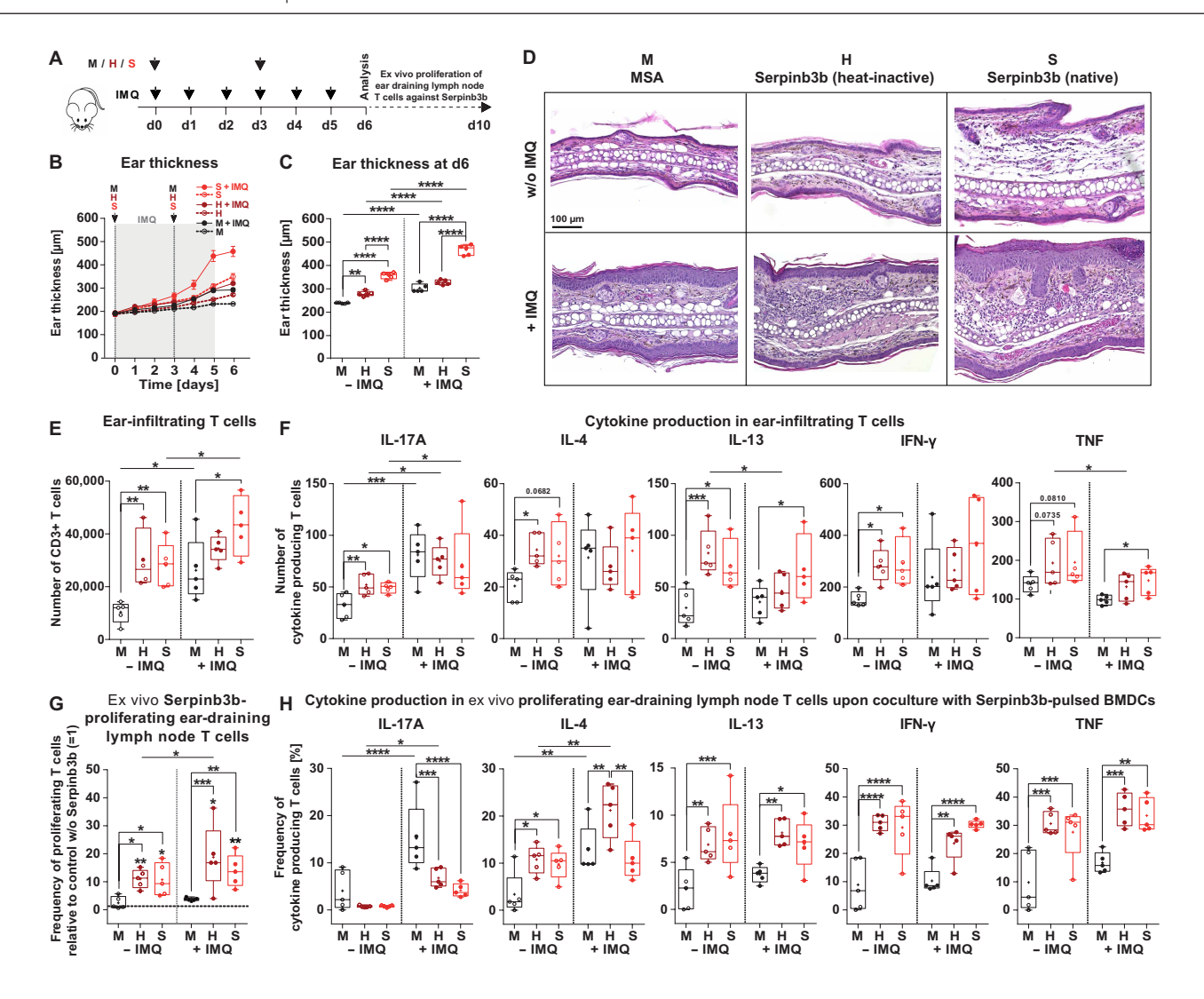


Fig. 2. Serpinb3b augments skin inflammation and induces an immune deviation toward a T_H2 /type 2 profile in vivo. (A) Experimental design: Mouse ears (n=5 per group, two independent experiments) were injected intradermally with 25 μ g of Serpinb3b [native (S), or heat-inactivated (H)] or murine serum albumin (MSA, control) on days 0 and 3. In addition, imiquimod (IMQ) cream was applied on the ear for six consecutive days from day 0 to day 5. Mice were euthanized on day 6. (B and C) Ear thickness was measured daily. (D) Representative H&E stainings of skin biopsies of the inflamed mouse ears. Scale bar, $100 \, \mu$ m. (E) Numbers of ear-infiltrating CD3⁺T cells on day 6 were determined by flow cytometry. (F) Frequencies of cytokine producing ear-infiltrating CD3⁺T cells were analyzed by flow cytometry. (G and H) Ex vivo Serpinb3b T cell proliferation assay: Ear-draining lymph node cells were isolated on day 6, CFSE stained, and cocultured for 4 days with bone marrow-derived dendritic cells (BMDCs), which were previously pulsed with Serpinb3b (10 μ g/ml) for 24 hours or left unstimulated (w/o antigen). Frequencies of proliferating CD3⁺T cells in coculture with Serpinb3b-stimulated BMDCs relative to those in coculture with unstimulated BMDCs (G) and their cytokine production (H) were determined by flow cytometry staining. Comparison within –IMQ or +IMQ mouse groups was performed using ordinary one-way ANOVA test. Comparison between –IMQ to +IMQ groups was performed using unpaired t test. *P < 0.05, **P < 0.01, ***P < 0.001, **, ative Serpinb3b; H, heat-inactivated Serpinb3b; M, MSA (murine serum albumin); IMQ, imiquimod; w/o, without.

cells from the MSA group (2.46 \pm 0.99% with P = 0.2131) showed no response (Fig. 2G). This effect was enhanced following the concomitant in vivo application of IMQ with proliferation reaching 13.88 \pm 2.57% (P = 0.0074) in the native Serpinb3b plus IMQ group and 18.78 \pm 5.17% (P = 0.0263) in the heat-inactivated Serpinb3b plus IMQ group. Because detection of Serpinb3b-reactive T cells was not expected in wild-type mice within 6 days of Serpinb3b injection without prior sensitization, we hypothesized that these mice had a preexisting pool of Serpinb3b-reactive T cells, e.g., triggered by previous undetected cutaneous injuries or subclinical skin inflammation. Activation-induced marker (AIM) multiplex assay indeed confirmed significantly higher frequencies of Serpinb3b-reactive T cells in lymph nodes and spleen of

wild-type mice after in vitro stimulation with heat-inactivated or native Serpinb3b, compared to MSA controls (fig. S4). These results support that wild-type mice may have a pool of Serpinb3b-reactive T cells.

Cytokine staining of ex vivo proliferating ear-draining lymph node T cells revealed a dominant T_H1/T_H2 immune pattern in Serpinb3b-reactive T cells with significantly increased frequencies of IL-4, IL-13, IFN- γ , and TNF-producing T cells in the native (P=0.0325, P=0.0008, P<0.0001, and P=0.0006) and heat-inactivated (P=0.0151, P=0.0041, P<0.0001, and P=0.0001) Serpinb3b groups compared to MSA (Fig. 2H). Injection of native or heat-inactivated Serpinb3b suppressed the frequency of IL-17A-producing proliferating T cells, which were only increased by the application of IMQ.

Together, our in vivo studies show that SERPINB3 is immunogenic and induces an immune deviation toward a mixed $T_{\rm H}1/T_{\rm H}2$ profile.

Serpinb3b drives amplification of Pso-like skin inflammation in vivo and induces TRMs

To next analyze the role of Serpinb3b for Pso development, we repeated experiments as shown in Fig. 2A (n = 5 per group) but analyzed the mice on day 18 (Fig. 3A). Consistent with the previous experiments, injection of Serpinb3b resulted in significantly increased ear swelling, with ear thickness being highest on day 6 $(349 \pm 7.1 \, \mu \text{m}, P < 0.0001)$, which was further enhanced by IMQ application (460 \pm 13.3 μ m, P < 0.0001) (Fig. 3, B and C). By day 18, inflammation decreased to baseline in all groups except in the Serpinb3b plus IMQ group (210 \pm 1.9 μ m, P < 0.0001), which still showed significantly higher ear thickness compared to the MSA plus IMQ (198 \pm 2.5 μ m) and Serpinb3b (193 \pm 3.0 μ m) groups (Fig. 3, B and D). Histology (Fig. 3E) and flow cytometry (Fig. 3F) on day 18 confirmed ear swelling and revealed high T cell infiltration in the Serpinb3b plus IMQ group (3737 \pm 150 cells) as well as a less prominent but still significantly increased T cell population in the Serpinb3b group (2304 \pm 318 cells, P = 0.0031) compared to MSA $(2059 \pm 287 \text{ cells}, P = 0.0009)$ and MSA plus IMQ $(1967 \pm 364 \text{ cells}, P = 0.0009)$ $P\!=\!0.0005)$ control groups. Serpinb3b-injected mice again displayed significantly higher frequencies of Serpinb3b-reactive T cells in the ear-draining lymph nodes (–IMQ: 3.7 \pm 0.27%, P < 0.0001; +IMQ: 3.5 \pm 0.24%, P = 0.0002) (Fig. 3G). Cytokine profiles of both ear-infiltrating T cells on day 18 (fig. S5A) and ex vivo Serpinb3b proliferating ear-draining lymph node T cells on day 22 (fig. S5B) again showed an immune deviation toward a $T_{\rm H}2/{\rm type}$ 2 profile.

Last, we investigated whether Serpinb3b induces TRMs that are known to contribute to chronification of inflammation. We found that the number of TRMs (CD3⁺CD69⁺CD103⁺) on day 18 was significantly higher in the Serpinb3b plus IMQ group (4392 \pm 261 cells, P < 0.0001) compared to the Serpinb3b (1335 \pm 139 cells) and MSA controls (–IMQ: 1370 \pm 184 cells; +IMQ: 1648 \pm 443 cells) (Fig. 3H). The Serpinb3b plus IMQ group also had the highest number of proliferating TRMs (CD3⁺CD69⁺CD103⁺Ki67⁺) (Fig. 3I), suggesting that Serpinb3b, especially when combined with IMQ, may promote chronic inflammation through TRM induction and maintenance.

The autoantigens SERPINB3 and SERPINB4 are linked to the psoriatic phenotype EczPso

In vivo murine experiments showed that Serpinb3b (i) stimulated skin inflammation, (ii) established cutaneous TRM populations, and

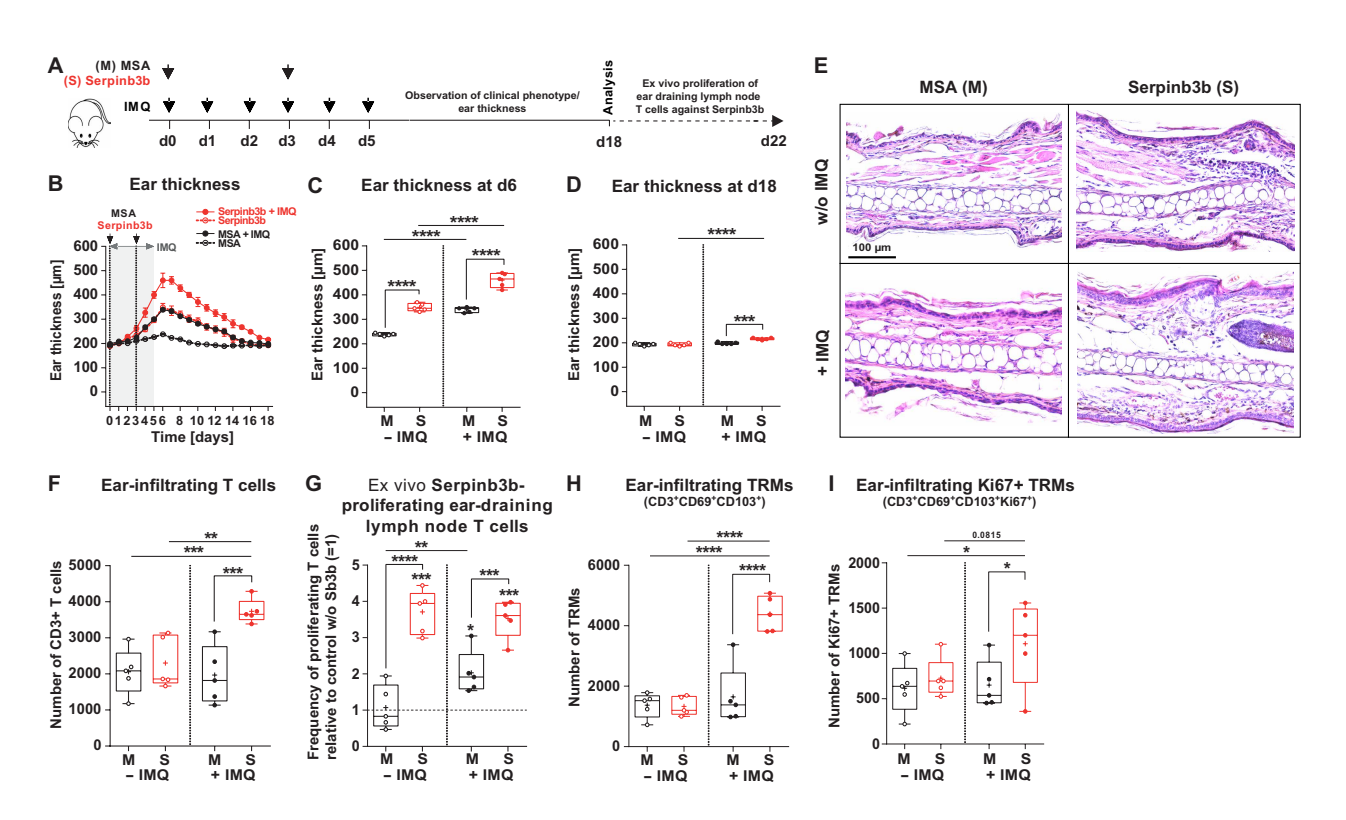


Fig. 3. Serpinb3b drives amplification of psoriasis-like skin inflammation in vivo and induces tissue-resident memory T cells. (A) Experimental design: Mouse ears (n = 5 per group, two independent experiments) were injected intradermally with 25 μ g of native Serpinb3b (S) or murine serum albumin (MSA, control) on days 0 and 3. In addition, imiquimod (IMQ) cream was applied on the ear for six consecutive days from days 0 to 5. Mice were euthanized on day 18. (**B** to **D**) Ear thickness was measured daily. (**E**) Representative H&E stainings of skin biopsies of the inflamed mouse ears on day 18. Scale bar, 100 μ m. (**F**) Numbers of ear-infiltrating CD3⁺T cells on day 18 were determined by flow cytometry. (**G**) Ex vivo Serpinb3b T cell proliferation assay: Ear-draining lymph node cells were isolated on day 18, CFSE stained, and cocultured for 4 days with bone marrow-derived dendritic cells (BMDCs), which were previously pulsed with Serpinb3b (10 μ g/ml) for 24 hours or left unstimulated (w/o antigen). Frequencies of proliferating CD3⁺T cells in coculture with Serpinb3b-stimulated BMDCs relative to those in coculture with unstimulated BMDCs were determined by flow cytometry staining. (**H** and **I**) Number of TRMs (CD3⁺CD69⁺CD103⁺) (H) and proliferating TRMs (CD3⁺CD69⁺CD103⁺Ki67⁺) (I) in the treated ears was analyzed by flow cytometry on day 18. Comparison within –IMQ or +IMQ mouse groups was performed using ordinary one-way ANOVA test. Comparison between the –IMQ to +IMQ groups was performed using unpaired t test. *P < 0.05, **P < 0.01, ***P < 0.001, ***P < 0.001, ***P < 0.0001. S, native Serpinb3b; M, MSA (murine serum albumin); IMQ, imiquimod; w/o, without; TRMs, tissue-resistant memory T cells.

(iii) shifted the immune response toward a T_H2 -phenotype, which is typically associated with eczema (Ecz). We therefore hypothesized that SERPINB3 may in particular play a pathogenic role for EczPso in humans, a subtype of Pso showing features of Ecz and T_H2 immunity (32). EczPso is defined as a chronic inflammatory skin disease that exhibits overlapping clinical, histological, and molecular features of both Pso and Ecz, making it diagnostically challenging. Following an

integrated multilayer diagnostic approach for the diagnosis of EczPso (fig. S6), histopathological analysis was performed in cases suspicious for the diagnosis of EczPso. Histopathological analysis of all skin samples used for immunopeptidome analyses identified classical plaquetype psoriasis vulgaris (PsV) in 6 patients, while 11 patients previously diagnosed with Pso but also exhibiting hallmarks of Ecz received the diagnosis of EczPso (Table 1). Representative histological

Table 1. Patient characteristics for the MS cohort and peptide counts for SERPINB3 and SERPINB4. Average values are shown as mean \pm SEM. EczPso, eczematized psoriasis; PsV, classical plaque-type psoriasis vulgaris; H, healthy; AUT, autopsy-derived skin; M, male; F, female.

	Clinical diagnosis	Histological diagnosis	Sex	Age	Peptide counts SERPINB3		Peptide counts SERPINB	
					HLA-I	HLA-II	HLA-I	HLA-II
Pso01_EczPso1	Psoriasis vulgaris	Eczematized psoriasis	М	46	1×		1×	
Pso04_EczPso2	Psoriasis vulgaris	Eczematized psoriasis	М	45		•	•	•••••
Pso05_EczPso3	Psoriasis vulgaris	Eczematized psoriasis	М	43		•	•	•••••
Pso07_EczPso4	Psoriasis vulgaris	Eczematized psoriasis	М	30	3×	•	3×	•••••
Pso08_EczPso5	Psoriasis vulgaris	Eczematized psoriasis	F	38	1×	•	1×	•••••
Pso11_EczPso6	Psoriasis vulgaris	Eczematized psoriasis	F	46	1×	4×	1×	2×
Pso12_EczPso7	Psoriasis vulgaris	Eczematized psoriasis	М	31		•		••••••
Pso13_EczPso8	Psoriasis vulgaris	Eczematized psoriasis	F	83		•••••		
Pso15_EczPso9	Psoriasis vulgaris	Eczematized psoriasis	М	33		•		
Pso17_EczPso10	Psoriasis vulgaris	Eczematized psoriasis	F	51	1×	7×	1×	8×
Pso02_EczPso11	Psoriasis vulgaris	Eczematized psoriasis	М	43	1×	•	1×	
Mean ± SEM (EczPso)		M: 7, F: 4,	44 ± 4.4	8×	11×	8×	10×	
Pso03_PsV1	Psoriasis vulgaris	Psoriasis vulgaris	F	40		•		•••••
Pso06_PsV2	Psoriasis vulgaris	Psoriasis vulgaris	М	44		•		•••••
Pso09_PsV3	Psoriasis vulgaris	Psoriasis vulgaris	М	51		•	•	
Pso10_PsV4	Psoriasis vulgaris	Psoriasis vulgaris	М	34		•	•	
Pso14_PsV5	Psoriasis vulgaris	Psoriasis vulgaris	М	43		•	•	
Pso16_PsV6	Psoriasis vulgaris	Psoriasis vulgaris	М	31	1×	•	1×	
Mean ± SEM (PsV)		M: 5, F: 1,	41 ± 2.9	1×	•	1×	•••••	
H1	Healthy	-	М	N/A		•	•	•••••
H2	Healthy	-	F	42		•	•	•••••
H3	Healthy	-	F	30			•	
H4	Healthy	-	F	62		•		
H5	Healthy	-	М	52		•		
H6	Healthy	-	М	28		•		
H7	Healthy	-	F	55		•		
H8	Healthy	-	М	26		•	•	•••••
H9	Healthy	-	F	51		• • • • • • • • • • • • • • • • • • • •	•••••	
H10	Healthy	-	F	26		• • • • • • • • • • • • • • • • • • • •	•••••	
Mean ± SEM (heal	lthy)		M: 4, F: 6,	41 ± 4.7		•	•	
AUT-DN04		-	F	47		2×		2×
AUT-DN05	•	-	М	90		•	•	
AUT-DN06	•	-	F	60		•••••		
AUT-DN08	•	-	М	59		•••••	•••••	
AUT-DN09	•••••••••••••	-	М	75		•	•••••	
AUT-DN11	•••••••••••••••••••••••••••••••••••••••	-	М	70				
AUT-DN12	***************************************	-	F	83				
AUT-DN13	***************************************	-	М	49		•••••	· 	
AUT-DN17		-	M	77		•••••	•••••	
Mean ± SEM (AUT	-DN)		· · · · · · · · · · · · · · · · · · ·	68 ± 5.0		2×	•••••	2×

images of patients with EczPso and PsV are shown in fig. S7A together with a patient with classical Ecz. An Ecz and Pso score based on histopathological criteria (33, 34) (Fig. 4A) to further quantify eczematous and Pso typical features showed a significantly higher Ecz score in patients diagnosed with EczPso (5.1 \pm 0.4 points, P < 0.0001) compared to those with PsV (1.5 \pm 0.4 points) (Fig. 4B). In contrast, the Pso score was lower in patients with EczPso (6.5 \pm 0.8 points, P = 0.0162) compared to those with PsV (9.7 \pm 0.8 points) (Fig. 4B).

Notably, the identified HLA class I- and HLA class II-presented SERPINB3 (Fig. 1D) and SERPINB4 (Fig. 1E) peptides were highly enriched in the skin of patients from the EczPso cohort. While SERPINB3 and SERPINB4 peptides were found in only 1 of 6 patients with PsV (17%) with only one peptide, 6 out of 11 patients with EczPso (54%) showed in total 19 unique SERPINB3 and SERPINB4 peptides (Fig. 4C). In more detail, only one HLA class I-presented SERPINB3 and SERPINB4 peptide was detected in one of six patients with PsV (PsV6). In contrast, seven distinct HLA class I- and 12 HLA class II-presented peptides derived from SERPINB3 as well as from SERPINB4 were eluted from 6 of the 11 patients with EczPso (EczPso 1, 4, 5, 6, 10, and 11). In conclusion, SERPINB3 and SERPINB4 peptides were predominantly presented in EczPso compared to PsV, suggesting a specific role for the autoantigens from SERPINB3 and SERPINB4 preferentially in the psoriatic subtype of EczPso.

EczPso harbors abundant SERPINB3 and is driven by $T_{\rm H}2/T_{\rm H}17$ cytokines

EczPso is an increasingly accepted clinical and histopathological subtype of Pso characterized by features of Ecz, because it is harder to treat with modern targeted therapies. Targeting Pso may lead to worsening of Ecz and vice versa (35, 36). Despite this unmet need, EczPso has been insufficiently studied at the cellular and molecular level and is not well understood. We analyzed lesional skin from patients with EczPso, PsV, and Ecz using immunohistochemistry (Fig. 4D) and bulk RNA sequencing (RNA-seq; fig. S7, B to D). IL-17A levels in EczPso were similar to those in PsV but much higher than those in Ecz. Ki67, a proliferation marker, and "neutrophil extracellular traps" (NETs) were lower in EczPso and Ecz, than in PsV, while FceRI⁺ cells characterizing Ecz were elevated in EczPso compared to PsV (Fig. 4D). Skin bulk RNA-seq showed a predominance of a T_H17/type 3 signature in EczPso, with Pso markers (e.g., IL17A, NOS2, and S100A7) up-regulated compared to Ecz (fig. S7, B and C). Gene set enrichment analysis confirmed both Ecz and Pso traits (fig. S7D). A molecular disease classifier (37) to quantitatively characterize EczPso at a molecular level based on the expression of NOS2 and CCL27 identified EczPso as primarily Pso with a lower probability for Pso than PsV (Fig. 4E). Thus, EczPso presents a mixed T_H2/T_H17 immune signature, confirming it as a Pso subtype with Ecz features.

To understand the role of SERPINB3 and EczPso, we first analyzed its expression by immunofluorescence staining. SERPINB3 levels were highest in the middle and upper epidermis of EczPso (567.4 \pm 117.7; median fluorescence of 605; n=9), compared to PsV (474.6 \pm 65.3; median fluorescence of 475; n=9) and Ecz (310.3 \pm 39.0; median fluorescence of 255; n=9) (Fig. 4F). SERPINB3 was detected in both intracellular and intercellular compartments in EczPso, whereas in PsV and Ecz, it was mainly seen intracellularly. Consistent with these findings, bulk RNA-seq demonstrated higher expression of *SERPINB3* and *SERPINB4* in EczPso and PsV compared to

Ecz (Fig. 4H). Spatial transcriptomics further confirmed that both SERPINB3 and SERPINB4 were most highly expressed across the upper, middle, and basal layers (fig. S8, A and B). To explore the upstream drivers of SERPINB3 expression, primary human keratinocytes were stimulated with T_H1, T_H2, and T_H17 cytokines. SERPINB3 mRNA (Fig. 4I) and protein levels (Fig. 4J) were significantly induced by IL-17A plus TNF (T_H17) and IL-4 (T_H2), with the highest induction observed when all three cytokines were combined, mimicking the T_H2/T_H17 cytokine milieu of EczPso skin. Spatial transcriptomics confirmed that SERPINB3 and SERPINB4 correlated strongly with IL13-, IL17A-, and combined IL13 + IL17Ainduced responder gene signatures, whereas correlations with IFNGinduced signatures were weaker within local tissue clusters (fig. S8C). In addition, SERPINB3 showed correlation with Pso-, and Ecz-specific marker genes, highlighting its role in disease-overlapping expression dynamics (fig. S8D).

Next, we evaluated how therapeutic inhibition of key cytokine pathways affects SERPINB3/SERPINB4 expression. Baricitinib, a JAK1/2 inhibitor used in Ecz treatment, which interferes with IL-4 signaling, reduced IL-4- but not IL-17A + TNF-induced SERPINB3 expression in human keratinocytes (fig. S9, A and B). Furthermore, baricitinib also suppressed SERPINB3 induction following stimulation with lesional T cell supernatants (TCS) isolated from PsV or Ecz skin biopsies or a mixture of both TSC (EczPso TSC) to mimic EczPso (fig. S9, C and D). Similarly, brodalumab, an IL-17 receptor inhibitor well established in Pso treatment, diminished SERPINB3 expression upon stimulation with EczPso TCS (fig. S9E). Similarly, both baricitinib and brodalumab interfered with SERPINB4 expression upon stimulation with the abovementioned cytokines and TCS (fig. S9, F to J). Immunoblotting confirmed our observations on the abrogated SERPINB3 protein expression upon treatment with baricitinib (fig. S9, K and L).

Lesional T cells from patients with EczPso proliferate upon SERPINB3 presentation and induces hallmarks of EczPso

Next, we wanted to better understand the spatial distribution of SERPINB3 and potentially SERPINB3-reactive T cells in EczPso. Therefore, we analyzed the colocalization of SERPINB3 and CD3⁺ T cells. We found increased CD3⁺ T cell colocalization with SERPINB3 in EczPso [6.8 \pm 1.6 cells per high-power field (HPF)] compared to PsV $(4.0 \pm 2.1 \text{ cells per HPF})$ and Ecz $(2.7 \pm 0.9 \text{ cells per HPF})$ (Fig. 5, A and B). Then, we isolated lesional T cells from skin biopsies of patients with EczPso (n = 10), PsV (n = 7), and Ecz (n = 5), cocultured them with autologous SERPINB3-pulsed monocyte-derived dendritic cells (MODCs) and measured SERPINB3-induced T cell proliferation compared to MODC stimulation without antigen. Only EczPso T cells showed significantly increased proliferation (P = 0.0020) upon SERPINB3 presentation (Fig. 5C and fig. S10). Comparing the relative frequencies to MODC stimulation without antigen (Fig. 5D), there were significantly more SERPINB3-reactive T cells in EczPso $(145.1 \pm 15.3\%, P = 0.0020)$, slightly less in PsV $(81.8 \pm 8.5\%,$ P = 0.0313), and unchanged in Ecz (102.6 ± 1.0, P = 0.0674). Of note, both CD4⁺ and CD8⁺ lesional T cells were activated by SERPINB3 in EczPso (Fig. 5E).

To eventually investigate whether SERPINB3-reactive T cells would contribute to the EczPso phenotype, reconstructed human epidermis (RHE) skin equivalents were stimulated with pooled lesional TCS mixes from EczPso, PsV, or Ecz. These supernatants were taken from the proliferation assays toward SERPINB3 of the respective lesional human

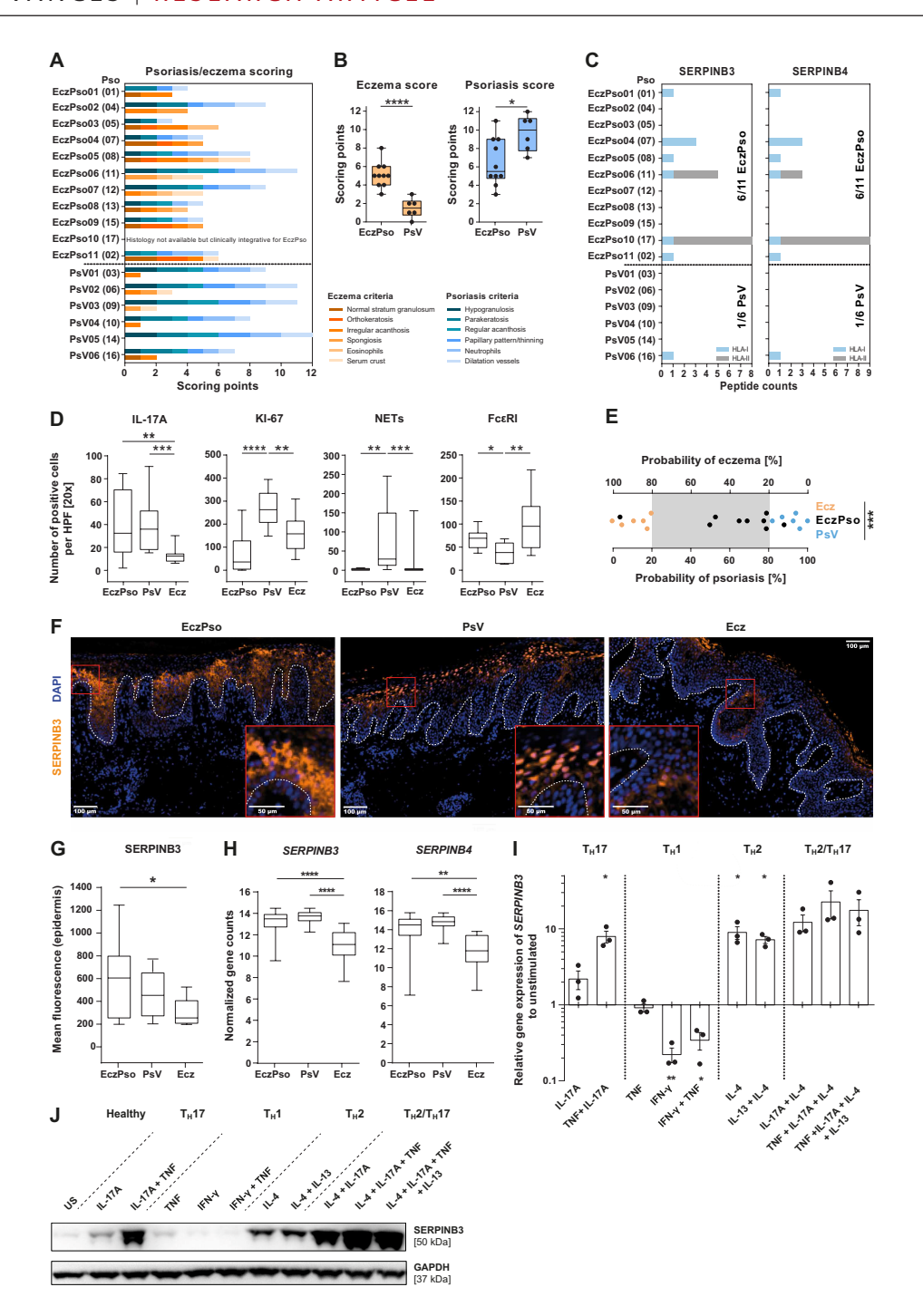


Fig. 4. The autoantigens SERPINB3 and SERPINB4 are linked to the psoriatic phenotype EczPso and are induced by T_H2/T_H17 cytokines. (A and B) Ecz and Pso scoring of H&E-stained Pso skin specimens from immunopeptidome analysis diagnosed histopathologically as either EczPso or PsV. Individual patient scores are shown in (A). Mean Ecz and Pso scores (B) were calculated for EczPso and PsV. Unpaired t test with Welch's correction. (C) Number of distinct HLA class I (blue) – and HLA class II (gray) – presented SERPINB3- and SERPINB4-derived peptide counts identified in patients with Pso separated into EczPso or PsV. (D) Number of positive cells per high-power field (HPF) at 20× for immunohistochemical stainings from patients with EczPso (n = 8), PsV (n = 14), and Ecz (n = 16). (E) Probability for Pso or Ecz in lesional skin of EczPso (n = 9), PsV (n = 6), and Ecz (n = 6) determined by the molecular classifier for Ecz and Pso (37). (F and G) Immunofluorescence staining of SERPINB3 in lesional skin of EczPso (n = 9), PsV (n = 9), and Ecz (n = 9). Representative images are shown in (F). Epidermal mean fluorescence of SERPINB3 is shown in (G). (H) Normalized gene counts of SERPINB3 and SERPINB4 in EczPso (n = 9), PsV (n = 34), and Ecz (n = 20) lesional skin determined by RNA-seq. (I and J) SERPINB3 expression in in vitro stimulated keratinocytes (n = 3) analyzed by qPCR (I) or Western blot (J). Data are visualized as mean \pm SEM. Ordinary one-way ANOVA test with Tukey's multiple comparison (for Gaussian distributed data) or nonparametric Kruskal-Wallis test with Dunn's multiple comparison (for non-Gaussian distributed data) was used to test for differences between disease groups. Comparison to unstimulated condition was performed using unpaired t test with Welch's correction (for Gaussian distributed data, D&I). *P < 0.05, **P < 0.01, ***P < 0.001, ****P < 0.0001. EczPso, eczematized psoriasis; PsV, classical plaque-type psoriasis vulgaris; Ecz, eczema; NETs, neutrophile extracellular t

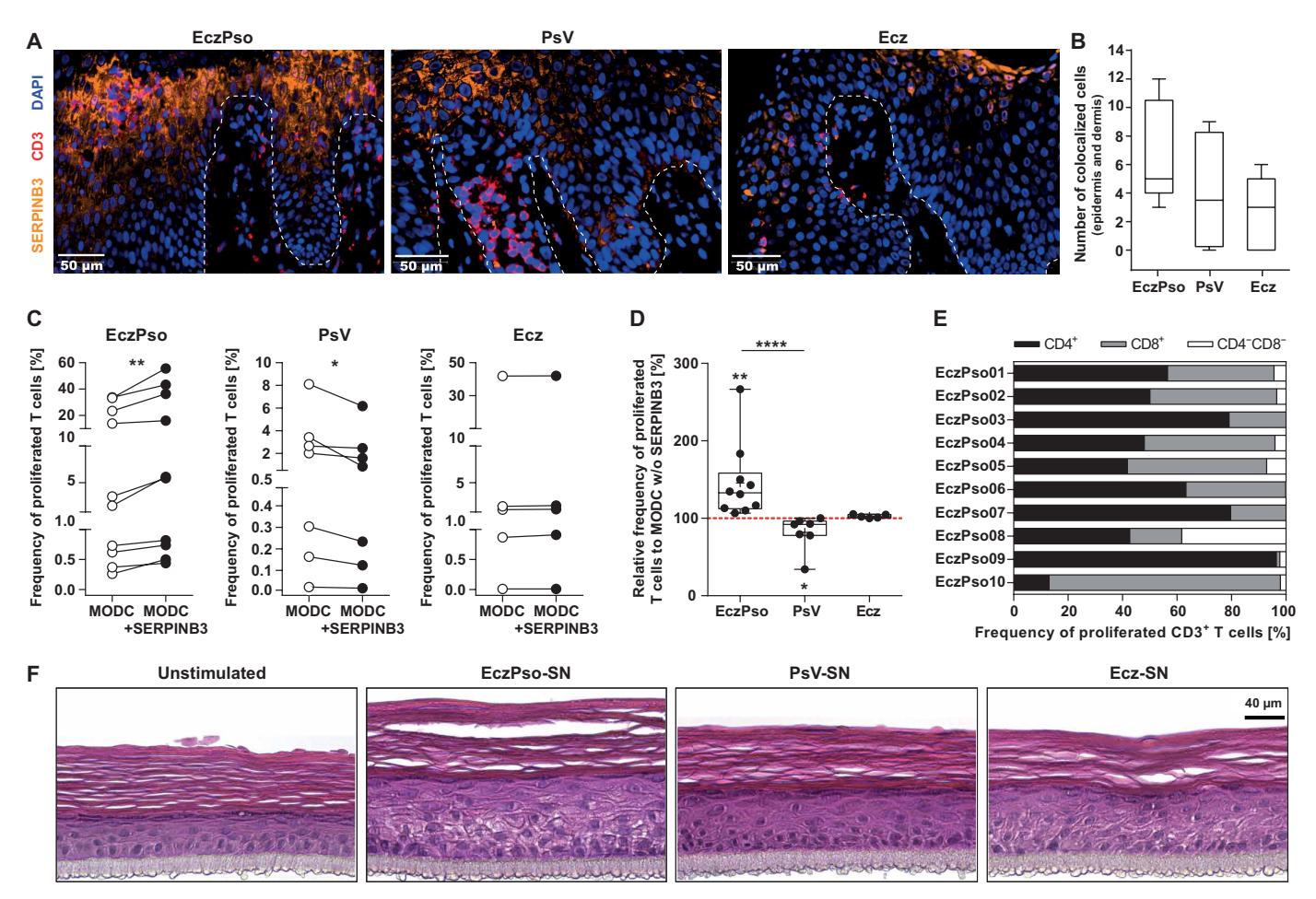


Fig. 5. Lesional T cells from patients with EczPso proliferate upon SERPINB3 and induces hallmarks of EczPso. (A and B) Immunofluorescent staining of lesional skin of EczPso (n = 9), and Ecz (n = 9) with SERPINB3 (orange) and CD3 (purple). Representative images are shown in (A). Nuclei were visualized by DAPI (blue). The dashed white line indicates the boundary between epidermis and dermis. Scale bar, 50 µm. The number of dermal and epidermal CD3⁺T cells colocalizing with SERPINB3 was quantified in (B). (C and D) Absolute (C) and relative (D) frequencies of SERPINB3-specific proliferating lesional CD3⁺T cells from patients with EczPso (n = 10), PsV (n = 7), and Ecz (n = 5) upon coculture with SERPINB3-pulsed autologous monocyte-derived dendritic cells (MODCs) determined by CFSE staining and flow cytometry. Relative frequencies (D) were normalized to the frequencies observed in cocultures with unstimulated MODCs. (E) Frequencies of CD4⁺ and CD8⁺T cells within the SERPINB3-proliferating CD3⁺T cells of patients with EczPso in (C) and (D). (F) H&E stainings of RHE skin equivalents (n = 1) stimulated for 72 hours with pooled lesional T cell supernatant from proliferating T cells shown in (C) for patients with EczPso (n = 10), PsV (n = 7), or Ecz (n = 5). Scale bar, 40 µm. Data are visualized as mean \pm SEM. Ordinary one-way ANOVA test with Tukey's multiple comparison (for Gaussian distributed data) or nonparametric Kruskal-Wallis test with Dunn's multiple comparison (for non-Gaussian distributed data) are visualized at test with Welch's correction (for Gaussian distributed data). *P < 0.05, **P < 0.05, **P < 0.00, ***P < 0.00, **P < 0.00, eczematized psoriasis; PsV, classical plaque-type psoriasis vulgaris; Ecz, eczema; MODC, monocyte-derived dendritic cells; w/o, without; RHE, reconstructed human epidermis; SN, supernatant; P < 0.00, value.

T cells. EczPso TCS displayed a predominant T_H2 profile with elevated T_H2 cytokines (e.g., IL-4, IL-9, and RANTES) and reduced T_H17 and T_H1 cytokines compared to PsV (fig. S11). RHE skin models treated with EczPso supernatants exhibited both spongiosis and acanthosis as seen in EczPso histopathology, whereas PsV supernatants induced only acanthosis (Fig. 5F). Analysis of bulk RNA-seq data from patients with various inflammatory skin diseases (n=261) confirmed that SERPINB3 and SERPINB4 expression strongly correlated with spongiosis, acanthosis (fig. S12A), and disease severity scores [Psoriasis Area and Severity Index (PASI) and Scoring Atopic Dermatitis (SCORAD)] (fig. S12B). Conversely, these genes negatively correlated with type 1–associated interface dermatitis (fig. S12A). These findings link SERPINB3 to the clinical and histological features of EczPso.

DISCUSSION

This study identifies SERPINB3 as a disease-relevant autoantigen in a clinically distinct Pso subtype, EczPso, characterized by overlapping T_H2 and T_H17 immune signatures. Through unbiased immunopeptidomics and functional validation in both murine and human models, we demonstrate that SERPINB3 drives inflammation, stimulates T cell proliferation, promotes TRMs, and induces hallmark features of EczPso. These findings reveal a mechanistic link between autoantigenicity and Pso heterogeneity, shedding light on the immunopathological basis of a clinically distinct disease subtype.

That SERPINB3 emerged as a detectable and disease-relevant autoantigen highlights its importance, even in the face of analytical constraints. Despite detecting fewer peptides than cancer studies

(22, 38), likely due to the lower abundance of HLA ligands in the skin and the small size of psoriatic tissue specimens (39), SERPINB3 remained detectable. This suggests that it is a prevalent and relevant HLA ligand in EczPso skin, while other Pso autoantigens may have been below the detection limit. In addition, LC-MS/MS systems used in this study lack the sensitivity, dynamic range, and acquisition speed characteristic of current state-of-the-art platforms. This reduced the overall peptidome coverage and impaired detection of low abundant peptides recovered from small tissue samples. Interindividual variability in SERPINB3/SERPINB4-derived peptide detection can thus arise from biological differences such as sample input, abundance of SERPINB3/SERPINB4-presenting cells within the analyzed biopsy, HLA presentation frequency per cell, and sample complexity, as well as technical factors including sample preparation efficiency and instrument sensitivity.

While PsV is the most common clinical phenotype, EczPso in contrast is an often neglected and less studied Pso subtype that accounts for an estimated 5 to 10% of patients with Pso (32). In addition to Pso characteristics, EczPso displays both clinical and histologic features of Ecz such as less demarcated plaques, irregular acanthosis, spongiosis, infiltrating eosinophils instead of neutrophils, and a serum crust. EczPso often poses a therapeutic challenge in modern targeted Pso therapies, indicating distinct immune pathways beside the IL-17 pathway (32). As SERPINB3 could be specifically linked to EczPso, we further characterized this subtype in a so far unprecedented depth. We demonstrated on both cellular and molecular level the mixed T_H2/type 2 and T_H17/type 3 signature underlying EczPso. Our results underpin why EczPso poses a therapeutic challenge particularly in the context of highly specific biologics and small-molecule inhibitors. Identification of SERPINB3 as a specific driver and biomarker in EczPso that also triggers chronification of inflammation in the respective patients may allow a better stratification of patients for more personalized treatment regimens. While individual peptide-specific T cell responses need to be unleashed or enhanced in cancer immunotherapy (40-42), the treatment of EczPso may, in contrast, benefit from approaches that modulate or dampen immune responses directed against SERPINB3 and SERPINB4. The recent success of CD19-targeted CAR T cell therapy in lupus erythematosus (43) illustrates that targeted therapies are being explored beyond oncology. Although still in early stages, antigen-specific CAR-regulatory T cell approaches (e.g., against SERPINB3) could, in principle, represent a future therapeutic strategy for inflammatory skin diseases with autoimmune features including subsets of Pso. Recently, mRNA-based vaccines have shown promising results in inducing antigen-specific tolerance in mouse models of autoimmune diseases such as multiple sclerosis (44). Whether such strategies might one day be adapted to chronic inflammatory skin diseases remains to be explored.

The previously described autoantigens LL37 and ADAMTSL5 have been demonstrated to be regulated by IL-17 (45), indicating a potential vicious cycle in which disease-relevant T cells produce cytokines that in turn induce the production of proteins activating T cells and thus inducing chronification of disease. In line with this, we demonstrated that SERPINB3 is abundantly present in the lesional Pso skin, particularly in EczPso and thus confirmed previous data showing overexpression of SERPINB3 and SERPINB4 in both the skin and serum of patients with Pso (46). Moreover, as shown for ADAMTSL5 and LL37 (47), we not only found an abundance of SERPINB3 in the Pso epidermis but also demonstrated its colocalization with immune

cells. Bassani-Sternberg et al. (48) showed a strong link between protein abundance and HLA presentation in several cell lines. Therefore, the marked production of proteins in inflamed keratinocytes may indeed create the potential for these proteins to be taken up by immune cells, to be presented via HLA molecules, and to consequently become targets for autoreactive T cells (47). While most human serpins are secreted proteins, SERPINB3 and SERPINB4 lack a signal peptide and are therefore primarily localized intracellularly under homeostatic conditions (24). The presence of SERPINB3 in intercellular compartments, which can be observed besides the intracellular SERPINB3 in EczPso skin, may result from both passive release from dying cells and active secretion by living cells, especially when expressed in high amounts. Both possibilities have been proposed in the literature (49, 50), but a definitive mechanism for SERPINB3 and SERPINB4 release remains to be established. Extracellular SERPINB3 and SER-PINB4 proteins can also be efficiently taken up by antigen-presenting cells and presented to SERPINB3- and SERPINB4-specific T cells.

With our murine experiments, we corroborated this hypothesis by showing that adding external Serpinb3b not only induced immune cell migration but also triggered the activation of T cells. As shown by Schabitz et al. (51), low numbers of pathogenic cytokine transcripts and their translated proteins can already promote disease pathogenesis by triggering local amplification cascades. Hence, even small numbers of SERPINB3-reactive T cells with their characteristic mixed T_H2 and T_H17 cytokine profile may be sufficient to drive the subtype of EczPso. Our experiments further showed that the effects of Serpinb3b were amplified in IMQ-treated skin. Given that IMQ is known to induce keratinocyte stress and damage, and Serpinb3b is localized in the cytosol, it is likely that IMQ increased the pool of immunogenic Serpinb3b peptides and thus the likelihood of Serpinb3b-reactive T cells. Moreover, we found that a mixture of T_H2/T_H17 cytokines strongly induces SERPINB3 expression in keratinocytes, which may thus lead to a self-amplifying loop, where SERPINB3 drives a shift toward a mixed T_H2/T_H17 milieu, which then further increases SERPINB expression. However, further in vivo studies, using, e.g., Serpinb3bdeficient mice, are needed to clarify whether SERPINB3 is necessary for the development of psoriatic inflammation.

Serpins regulate key proteolytic processes in inflammation, immune tolerance, and tissue homeostasis and have been proposed as autoantigens in autoimmune and inflammatory diseases: Anti-serpin E2 autoantibodies were identified in rheumatoid arthritis (52) and SerpinB13 antibodies have been shown to promote β cell development and resistance to type 1 diabetes (53). Conformational changes during serpin protease activity may expose cryptic epitopes, triggering autoantibody formation. In addition, misfolded or modified serpins may accumulate and drive persistent inflammation through chronic immune activation (54). In Pso, the serpin-derived peptide Pso p27 was suggested as a putative autoantigen, being present exclusively in lesional but not in nonlesional skin. Its abundance correlated with disease activity, and it formed large aggregates with potentially immunogenic properties (18, 55). Our study extends these findings by identifying SERPINB3- and SERPINB4derived HLA peptides which include but are not limited to Pso p27 sequences, suggesting a larger pool of serpin-derived autoantigens than previously recognized. It was previously shown that Pso27 is generated from SERPINB3 cleavage in the presence of mast cell-associated chymase (56). Combined with our immunofluorescence data showing increased intercellular epidermal localization of SERPINB3 and also more abundant expression of FceRI—a master regulator of mast cells (57) in Ecz and EczPso than in PsV, this raises the possibility that mast cells

internalize SERPINB3 and contribute to antigen processing and presentation particularly in EczPso. This is also supported by previously published data showing correlation between the number of mast cells and disease severity in Ecz (58) and the identification of mast cells as key sources of Ecz cytokines IL-4 and IL-13 (59). While none of the identified HLA-presented peptides in our study spanned the cleavage site of mast cell–associated chymase, mast cells may still be involved in processing SERPINB3 and SERPINB4 epitopes in EczPso, given their capacity to process and present antigens via HLA molecules and the enhanced expression of immunogenic SERPINB3 and SERPINB4 in a mixed $T_{\rm H}2/T_{\rm H}17$ cytokine milieu.

SERPINB3 and SERPINB4 show high sequence homology; however, we could identify SERPINB4-specific peptides that are not homologous to SERPINB3 in almost equal amounts to those specific to SERPINB3 in our patients. Therefore, we speculate that both proteins function as de facto autoantigens. However, patient samples containing peptides specific to SERPINB3 also contain peptides specific to SERPINB4, and the difference in peptide sequence is often only one amino acid, which strongly argues for T cell cross-reactivity. Nevertheless, future studies are necessary to demonstrate the immunogenicity of SERPINB4. SERPINB4, similarly to SERPINB3, is highly expressed in lesional psoriatic skin, but given its distinct substrate specificity, its putative functional role in Pso pathogenesis warrants further investigations.

We demonstrated that the injection of Serpinb3b in both its native and heat-inactivated form augmented the inflammation induced by IMQ application. Because heat inactivation abolishes catalytic activity, we speculate that residual structural epitopes may account for the pronounced in vivo activity observed with heat-inactivated Serpinb3b. Nevertheless, native Serpinb3b induced a more pronounced inflammation than the heat-inactivated form. One explanation is that the protein's inhibitory function or potentially other direct proinflammatory activities contribute to skin inflammation, and these functions are lost upon heat-inactivation. Overexpression of SERPINB3 and SER-PINB4 in the HaCatT immortalized keratinocyte cell line has been reported to activate NF-kB transcription factors, thereby inducing the expression of various cytokines (e.g., CXCL1, CXCL8, and IL-1B) and chemokines (e.g., CCL20). Moreover, in vivo knockdown of Serpinb3a, another murine ortholog of SERPINB3, was shown to alleviate IMQinduced skin inflammation (60). However, the exact molecular pathways involved and whether they depend on the protease inhibitor functions of SERPINB3 and SERPINB4 remain to be elucidated. An additional, possibly complementary explanation for the more pronounced inflammation induced by the injection of native Serpinb3b may relate to its role as an autoantigen. Specifically, heat-induced conformational changes might disrupt epitopes that are recognized by T cells. Serpinb3b injection promoted the generation of TRMs in vivo. TRMs have been implicated in driving the chronic nature of Pso, suggesting their central role in disease persistence (61). Therapeutic approaches currently provide symptom relief only while treatment is ongoing, without achieving a definitive cure. A key challenge remains the recurrence of disease following therapy withdrawal (62). Emerging evidence indicates that patients with a shorter disease history experience longer remission periods when treated early, possibly by preventing the formation of TRMs and thus disease chronification as a pivotal strategy for achieving sustained disease resolution or cure (63, 64). These findings suggest that early targeting of SERPINB3 as outlined above may represent a promising strategy to prevent disease chronification, particularly in the subset of patients with EczPso.

Together, we provide evidence that SERPINB3 and SERPINB4 peptides are associated with EczPso and that SERPINB3 may be a specific autoantigen in a subcohort of patients with Pso.

MATERIALS AND METHODS

Study cohort and ethic compliance

All human specimens were collected in accordance with the Declaration of Helsinki protocol and local ethics committees: Klinikum Rechts der Isar (44/16S and 5590/12) and Cantonal Ethics Committee Zürich (KEK) (BASEC-Nr. Req-2016-00604) (39). Punch biopsies (6 mm) of lesional and nonlesional skin were collected under local anesthesia. To ensure a clear diagnosis, clinical as well as histological assessment was performed by independent dermatologists as well as dermato-pathologists. All patients gave their written informed consent. For mass spectrometry, psoriatic (n = 17 with Ecz-Pso n = 10 and PsV n = 7) and healthy control skin biopsies (n = 10) were collected. Postmortem autopsy-derived skin samples (n = 9)complemented the healthy dataset (39). Patient characteristics of the mass spectrometry cohort are listed in Table 1. For proliferation assay, RNA-seq, immunohistochemistry (IHC), immunofluorescence (IF), and classifier, EczPso, PsV, and Ecz skin biopsies were collected (proliferation: 10/7/5, IHC: 8/14/16, IF: 9/9/9, RNA-seq: 9/34/20, and classifier: 9/6/6). Each biopsy was divided into three parts: One part was fixed in 4% formalin for histology, one part was collected in RNAlater Stabilization Solution (Qiagen) at -80°C until RNA preparation and one part was directly used for the isolation of lesional T cells. Patient characteristics of the proliferation assay cohort are listed in Table 2. Patient characteristics of the RNA-seq cohort are listed in table S2.

Histopathological evaluation

Hematoxylin and eosin (H&E)-stained skin specimens were diagnosed by two dermatopathologists in the course of routine histopathological analysis. In addition, specimens were scored according to a modified published Pso and Ecz score to evaluate histologic similarity to Pso or Ecz (33, 34). Each criterion (fig. S6) was scored separately: Absence of a characteristic was scored as 0 point, mild presence of the characteristic was scored as 1 point, and severe presence of the characteristic was scored as 2 points. Thus, a maximum of 12 points could be achieved for both scores.

Mass spectrometry of immunoaffinity-purified HLA ligands Isolation of HLA ligands

HLA class I and II ligands were isolated and analyzed as described previously (39, 65). In brief, standard immunoaffinity chromatography using the pan-HLA class I–specific monoclonal antibody W6/32 (66), the pan-HLA class II–specific antibody Tü39 (67), and the HLA-DR–specific antibody L243 (68) (all produced in-house at the Department of Immunology, University of Tübingen) was performed from tissue lysates prepared from fresh frozen tissue. Psoriatic Pso17_EczPso10 and healthy H01 specimens were additionally digested with collagenase before HLA ligand isolation.

Identification by LC-MC/MS

Mass spectrometric data were acquired on an LTQ Orbitrap XL and/ or an Orbitrap Fusion Lumos (both from Thermo Fisher Scientific) as described previously (39, 69). Subsequent database search against the Swiss-Prot database (released from 27 September 2013) was performed using the SEQUEST search algorithm (70) embedded as

Table 2. Patient characteristics for the SERPINB3 T cell proliferation cohort and proliferation frequencies upon SERPINB3 stimulation. Average values are shown as mean \pm SEM. EczPso, eczematized psoriasis; PsV, classical plaque-type psoriasis vulgaris; Ecz, eczema; M, male; F, female.

	Clinical diagnosis	Histological diagnosis	Sex	Age	SERPINB3 proliferated CD3 ⁺ T cells to w/o antigen (%)	Frequency CD3 ⁺ CD4 ⁺ (%)	Frequency CD3 ⁺ CD8 ⁺ (%)
EczPso1	Psoriasis vulgaris	Eczematized psoriasis	М	55	116.5	56.5	39.1
EczPso2	Psoriasis vulgaris	Eczematized psoriasis	М	50	179.3	50.0	46.6
EczPso3	Psoriasis vulgaris	Eczematized psoriasis	М	60	142.9	79.1	20.9
EczPso4	Psoriasis vulgaris	Eczematized psoriasis	М	54	266.7	48.0	48.0
EczPso5	Psoriasis vulgaris	Eczematized psoriasis	М	52	110.0	41.7	51.2
EczPso6	Psoriasis vulgaris	Eczematized psoriasis	М	46	150.0	63.3	36.6
EczPso7	Psoriasis vulgaris	Eczematized psoriasis	F	63	113.2	79.6	20.4
EczPso8	Psoriasis vulgaris	Eczematized psoriasis	М	69	131.2	42.6	19.1
EczPso9	Psoriasis vulgaris	Eczematized psoriasis	F	48	106.7	96.5	1.3
EczPso10	Psoriasis vulgaris	Eczematized psoriasis	F	48	134.5	13.0	85.0
Mean ± SEM	l (EczPso)		M: 7, F: 3,	, 55 <u>+</u> 2.3	145.1 <u>+</u> 15.3		•
PsV1	Psoriasis vulgaris	Psoriasis vulgaris	F	40	77.8		•
PsV2	Psoriasis vulgaris	Psoriasis vulgaris	М	37	92.9		•
PsV3	Psoriasis vulgaris	Psoriasis vulgaris	F	68	79.3		•
PsV4	Psoriasis vulgaris	Psoriasis vulgaris	F	56	100.0		•••
PsV5	Psoriasis vulgaris	Psoriasis vulgaris	F	29	92.2		•••
PsV6	Psoriasis vulgaris	Psoriasis vulgaris	М	39	34.2		•
PsV7	Psoriasis vulgaris	Psoriasis vulgaris	М	24	96.4		•
Mean ± SEM	l (PsV)		M: 3, F: 4,	42 ± 5.8	81.1 <u>+</u> 8.5		•
Ecz1	Eczema	Eczema	М	51	105.3		•
Ecz2	Eczema	Eczema	F	49	100.0		•
Ecz 3	Eczema	Eczema	М	46	104.6		
Ecz 4	Eczema	Eczema	М	53	102.2		
Ecz 5	Eczema	Eczema	М	80	100.8		•
Mean ± SEM (Ecz)		M: 4, F: 1, 56 ± 6.2		102.6 ± 1.0		•	

processing node in Proteome Discoverer 1.4 (Thermo Fisher Scientific) at \leq 5% false discovery rate. Oxidation of methionine residues was permitted as dynamic modification. Healthy specimen H01 was processed and measured as biological triplicates, and the data were merged for downstream analysis.

Human T cell proliferation assay Isolation of lesional T cells

Lesional T cells were isolated from freshly taken skin biopsies by emigration toward an IL-2 (60 U, Proleukin) gradient followed by expansion with α -CD3 (BD, 555329, 0.75 μ g/ml, coated) and α -CD28 (BD, 55572, 0.75 μ g/ml) stimulation as described previously (71, 72). Before coculture with MODCs, T cells were stained with CFSE (Thermo Fisher Scientific, C34554, 1 μ M) according to the manufacturer's instructions.

Monocyte isolation and MODC generation

PBMCs were isolated from patients' peripheral blood using Lympho-Prep (Progen Biotek, 1114547) and were magnetically separated for CD14⁺ cells using human CD14 MicroBeads (Miltenyi Biotec, 130-050201) with the autoMACS Pro Separator (Miltenyi Biotec, 130-092-545). Monocytes were then differentiated into MODCs for 7 days in the presence of granulocyte-macrophage colony-stimulating factor (GM-CSF; Miltenyi Biotec, 130-093-864, 150 U/ml) and IL-4 (Miltenyi

Biotec, 130-093-920, 150 U/ml) as described previously (71). Before coculture with lesional T cells, differentiated MODCs were stimulated for 24 hours with rhSERPINB3 protein (10 μ g/ml; Novoprotein, CJ63) or rhTetanus toxoid (10 μ g/ml; Enzo Life Sciences, ALX-630-108-C100) as positive control or w/o antigen as negative control.

T cell proliferation assay

Proliferation assays were performed by 10-day coculturing of 2.5×10^4 antigen-pulsed autologous MODCs with 5×10^5 CFSE-labeled lesional T cells followed by flow cytometry analysis [CD3 (BV711, BioLegend, 317327, clone Okt3, 1:100), CD4 (AF700, BioLegend, 300526, clone RPA-T4, 1:500), and CD8 (APC-H7, BD, 561423, clone SK1, 1:50)] to determine the frequencies of SERPINB3-reactive T cells as previously described (71). For pulsing, MODCs were incubated with recombinant SERPINB3 (10 $\mu g/ml)$ for 24 hours. Patient characteristics of the proliferation cohort are listed in Table 2, and representative CFSE tracings of SERPINB3-proliferated T cell frequencies are shown in fig. S10.

In vivo Serpinb3b mouse model Experimentally induced Pso-like dermatitis and Serpinb3bsensibilization model

All animal work was conducted in accordance with the German Federal Animal Protection Laws and approved by the government of Upper Bavaria (Regierung von Oberbayern, Munich, Germany, ROB-55.2-2532.Vet_02-20-222). C57Bl6/J female mice (8 to 16 weeks old; n=5 per group) were obtained from Charles River Laboratories and used for animal experiments. Recombinant murine Serpinb3b [25 µg; S, high-purity endotoxin-free in-house production (see Supplementary Methods)] or heat-inactivated (90°C for 10 min) Sb3b (H), both solved in 20 µl of phosphate-buffered saline (PBS) or MSA (M; Merck, A3559-5MG) as control was injected intradermally into the left ear on days 0 and 3. In addition, Aldara (5% IMQ cream, MEDA Pharmaceuticals) was applied topically daily to the left ear from day 0 to day 5. Ear thickness was measured using a digital micrometer. Mice were euthanized on day 6 or 18. Two independent experiments were performed in each case.

Isolation of ear-infiltrating immune cells

For the analysis of ear-infiltrating immune cells, the ears were processed as previously described (73) on day 6 or 18. Dorsal and ventral parts of the ears were separated, followed by brief digestion with dispase II (Sigma-Aldrich) and collagenase and DNase I (both from Roche). The tissues were filtered through a 70- μ m nylon mesh and the single-cell suspensions were separated using Percoll density gradient centrifugation. The isolated cell suspensions were stimulated for 4 hours at 37°C with a Cell Activation Cocktail (BioLegend, 423303) following flow cytometry analysis.

T cell proliferation assay

BMDCs were derived from bone marrow cells of 8-week-old C57Bl6/J mice as previously described (74). Bone marrow cells were plated into 100-mm petri dishes in complete differentiation medium [RPMI (Gibco) supplemented with 10% fetal calf serum (Hyclone), 5×10^5 M 2-ME, penicillin G (100 IU/ml), streptomycin sulfate (100 IU/ml), and GM-CSF (200 U/ml) (PeproTech)]. Seven days later, BMDCs were stimulated with Serpinb3b (10 µg/ml) for 24 hours. On day 6 or 18, ear-draining lymph nodes from the left side were isolated and mashed, filtered through a 70-µm nylon mesh and stained with CFSE (Thermo Fisher Scientific, C34554, 1 µM). Then 2×10^5 CFSE-stained ear-draining lymph node cells were cocultured with 1×10^4 Serpinb3b-pulsed BMDCs for 4 days. On day 4, cocultures were restimulated for 5 hours with phorbol 12-myristate 13-acetate (PMA) (Sigma-Aldrich, P8139, 10 ng/ml), ionomycin (Sigma-Aldrich, I0634, 1 µg/ml), GolgiStop (BD, 554724, 1:1500), and GolgiPlug (BD, 555029, 1:1000, only the last 3 hours) following flow cytometry analysis.

AIM multiplex assay

The previously published multiplexed AIM assay (75) was adapted to identify Serpinb3b-specific CD4⁺T cells. Lymph node and spleen immune cells were isolated from C57BL/6 wild-type mice (n=5) and stimulated in vitro on day 0 with recombinant native or heatinactivated Serpinb3b (S, H), or MSA as a control (each 10 µg/ml). After an initial resting period, a second in vitro stimulation was performed on day 7 for 15 hours following flow cytometry analysis.

Flow cytometry analysis of mouse cells

For flow cytometry analysis, cells were first stained with LIVE/DEAD Fixable Near IR (Invitrogen, L34980, 1:1000) or LIVE/Dead Fixable Aqua (Invitrogen, L34957, 1:1000) to assess viability. Following blocking with anti-CD16/32 (BioLegend, 101320, 1:250) to prevent nonspecific binding, the following surface markers were stained: CD3ɛ (BV605, BioLegend, 100351, 1:100), CD8 (Pacific Blue, BioLegend, 100725, 1:600), CD4 (FITC, BioLegend, 100406, 1:400 or BV421, BioLegend, 100438, 1:500 or APC, BioLegend, 100412, 1:250), CD69 (AF700, BioLegend, 104539, 1:125), CD103 (FITC, BioLegend,

121419, 1:125), CD45 (BV510, BioLegend, 103138, 1:250), CD44 (APC-EFluor780, eBioscience, 47-0441-82, 1:100), CD137 (4-1BB) (eFluor450, Invitrogen, 48-1371-82, 1:250), CD134 (OX40) (PE-Cy7, BioLegend, 119416, 1:100), and CD154 (CD40L) (PE/Dazzle 594, BioLegend, 157015, 1:250). For intracellular cytokine staining, the cells were then fixed in formalin:PBS (1:1, 40 min, room temperature) and permeabilized using perm buffer (Invitrogen, 00-8333-56). The following intracellular markers were stained: IL-17A (APC-Cy7, Bio-Legend, 506940, 1:400), IL-4 (APC, BD, 554436, 1:250), IL-13 (PE, eBioscience, 12-7133-81, 1:250), IFN-γ (PE-Cy7, BioLegend, 505826, 1:250), TNF (PerCP-Cy5.5, BioLegend, 506321, 1:250), and Ki67 (BV650, BioLegend, 151215, 1:250). Data were collected with an LSR Fortessa (BD) or CytoFLEX LX flow cytometer (Beckman Coulter) and analyzed using FlowJo V10 software (www.flowjo.com). For the AIM assay, gating strategies were applied using Boolean AND/OR combinations for data subset identification.

Culture and stimulation of primary human keratinocytes

Primary human epidermal keratinocytes were obtained by suction blister as reported before (34) and cultured in keratinocyte medium [DermaLife Basal Medium supplemented with DermaLife K LifeFactor Kit (Lifeline Cell Technology, LL-0007)] at 37°C, 5% CO₂. Characteristics of healthy keratinocyte donors are listed in table S3. Second-to third-passage primary human epidermal keratinocytes were used and cultured in tissue culture–treated six-well plates with a starting cell number of 0.2×10^6 . For stimulation, cells were starved for 5 hours in DermaLife Basal Medium following stimulation with human recombinant IL-17A (R&D Systems, 317-ILB-050, 50 ng/ml), TNF [R&D Systems, 210_TA-005, 10 (when in combination) or 50 ng/ml (single stimulation)], IFN- γ (R&D Systems, 285-IF-100/CF, 50 ng/ml), IL-4 (Miltenyi Biotec, 130-093-921, 50 ng/ml), or IL-13 (R&D Systems, 213-ILB-005, 50 ng/ml) for 16 hours (RNA analysis) or 72 hours (WB analysis) in keratinocyte medium without hydrocortisone.

RHE skin equivalents

RHE skin equivalents were cultured in collagen-coated (1% Collagen type I in PBS, Sigma-Aldrich, C3867-1VL) polycarbonate inserts (Millipore, PIHP01250) as described previously (76). A total of 0.3×10^6 primary human keratinocytes were seeded in 500 µl of keratinocyte medium supplemented with 1.5 mM CaCl₂ (Sigma-Aldrich, C-7902) into the insert. Characteristics of healthy keratinocyte donors are listed in table S3. Keratinocyte medium (2.5 ml) + 1.5 mM CaCl₂ was added in the surrounding well. Models were cultured at 37°C and 5% CO₂. Two days after seeding, airlift was done by aspirating the medium in the insert, and the medium in the surrounding 6-well was replaced with 1.8 ml of keratinocyte medium + 1.5 mM CaCl₂ + vitamin C (50 μg/ml; Sigma-Aldrich, A5960-25G). Every second to third day, the medium in the surrounding 6-well was replaced with 2 ml of keratinocyte medium + 1.5 mM CaCl₂ + vitamin C (50 μg/ml). Nine days after airlift, RHE skin equivalents were stimulated with proliferation assayderived TCS 1:10 diluted in 2 ml of keratinocyte medium without hydrocortisone + 1.5 mM $CaCl_2$ + vitamin C (50 μ g/ml) for 3 days. For histology, inserts were fixated with 4% formaldehyde (Fischar, 27244) for 24 hours at 4°C. Afterward, membranes of the fixated RHE skin equivalents were cut out with a scalpel, divided into two pieces, and embedded in paraffin. Sections (5 μm) were cut and dewaxed at 65°C for 20 min. After rehydration, sections were stained with H&E using standard methods. High-resolution images (20x) were obtained with an Evos microscope.

Statistical analysis

All experiments were performed in biological replicates (number indicated in text and figure legends) unless otherwise indicated. Data were analyzed using GraphPad Prism 6 software and visualized as mean \pm SEM or as boxplot. For significance analysis, datasets were first tested for Gaussian distribution using Shapiro-Wilk test. To test for differences in the mean value within disease groups, the parametric ordinary one-way analysis of variance (ANOVA) test with Tukey's multiple comparison (for Gaussian distributed data) or the nonparametric Kruskal-Wallis test with Dunn's multiple comparison (for non-Gaussian distributed data) was used. Comparison of mean values relative to unstimulated conditions was performed using an unpaired two-sided t test with Welch's correction (for Gaussian distributed data) or the Wilcoxon test (for non-Gaussian distributed data). Significance level was defined as *P < 0.05, **P < 0.01, ***P < 0.001, and ****P < 0.0001.

Supplementary Materials

The PDF file includes:

Supplementary Materials and Methods Figs. S1 to S13 Tables S1 to S4 Legends for files S1 and S2 References

Other Supplementary Material for this manuscript includes the following: Files S1 and S2

REFERENCES AND NOTES

- P. Sewerin, R. Brinks, M. Schneider, I. Haase, S. Vordenbaumen, Prevalence and incidence of psoriasis and psoriatic arthritis. Ann. Rheum. Dis. 78, 286–287 (2019).
- R. Parisi, D. P. Symmons, C. E. Griffiths, D. M. Ashcroft, Identification and Management of Psoriasis Associated ComorbidiTy (IMPACT) project team, Global epidemiology of psoriasis: A systematic review of incidence and prevalence. *J. Invest. Dermatol.* 133, 377–385 (2013).
- E. Christophers, Explaining phenotype heterogeneity in patients with psoriasis. Br. J. Dermatol. 158, 437–441 (2008).
- A. R. Noorily, M. C. Criscito, J. M. Cohen, N. K. Brinster, Psoriasis with eczematous features: A retrospective clinicopathologic study. *Am. J. Dermatopathol.* 43, 112–118 (2021).
- C. E. M. Griffiths, A. W. Armstrong, J. E. Gudjonsson, J. Barker, Psoriasis. Lancet 397, 1301–1315 (2021).
- C. W. Lynde, Y. Poulin, R. Vender, M. Bourcier, S. Khalil, Interleukin 17A: Toward a new understanding of psoriasis pathogenesis. J. Am. Acad. Dermatol. 71, 141–150 (2014).
- A. Di Cesare, P. Di Meglio, F. O. Nestle, The IL-23/Th17 axis in the immunopathogenesis of psoriasis. J. Invest. Dermatol. 129, 1339–1350 (2009).
- A. Sharma, D. K. Upadhyay, G. D. Gupta, R. K. Narang, V. K. Rai, IL-23/Th17 axis: A potential therapeutic target of psoriasis. *Curr. Drug Res. Rev.* 14, 24–36 (2022).
- R. G. Langley, B. E. Elewski, M. Lebwohl, K. Reich, C. E. Griffiths, K. Papp, L. Puig, H. Nakagawa, L. Spelman, B. Sigurgeirsson, E. Rivas, T. F. Tsai, N. Wasel, S. Tyring, T. Salko, I. Hampele, M. Notter, A. Karpov, S. Helou, C. Papavassilis, ERASURE Study Group, FIXTURE Study Group, Secukinumab in plaque psoriasis—Results of two phase 3 trials. N. Enal. J. Med. 371. 326–338 (2014).
- C. Leonardi, R. Matheson, C. Zachariae, G. Cameron, L. Li, E. Edson-Heredia, D. Braun, S. Banerjee, Anti-interleukin-17 monoclonal antibody ixekizumab in chronic plaque psoriasis. N. Engl. J. Med. 366, 1190–1199 (2012).
- K. A. Papp, J. F. Merola, A. B. Gottlieb, C. E. M. Griffiths, N. Cross, L. Peterson, C. Cioffi, A. Blauvelt, Dual neutralization of both interleukin 17A and interleukin 17F with bimekizumab in patients with psoriasis: Results from BE ABLE 1, a 12-week randomized, double-blinded, placebo-controlled phase 2b trial. J. Am. Acad. Dermatol. 79, 277–286. e10 (2018).
- K. A. Papp, C. Leonardi, A. Menter, J. P. Ortonne, J. G. Krueger, G. Kricorian, G. Aras, J. Li,
 C. B. Russell, E. H. Thompson, S. Baumgartner, Brodalumab, an anti-interleukin-17-receptor antibody for psoriasis. *N. Engl. J. Med.* 366, 1181–1189 (2012).
- R. P. Nair, P. E. Stuart, I. Nistor, R. Hiremagalore, N. V. C. Chia, S. Jenisch, M. Weichenthal, G. R. Abecasis, H. W. Lim, E. Christophers, J. J. Voorhees, J. T. Elder, Sequence and

- haplotype analysis supports HLA-C as the psoriasis susceptibility 1 gene. Am. J. Hum. Genet. **78**, 827–851 (2006).
- Z. Shen, G. Wang, J. Y. Fan, W. Li, Y. F. Liu, HLA DR B1*04, *07-restricted epitopes on keratin 17 for autoreactive T cells in psoriasis. J. Dermatol. Sci. 38, 25–39 (2005).
- R. Lande, E. Botti, C. Jandus, D. Dojcinovic, G. Fanelli, C. Conrad, G. Chamilos, L. Feldmeyer,
 B. Marinari, S. Chon, L. Vence, V. Riccieri, P. Guillaume, A. A. Navarini, P. Romero,
 A. Costanzo, E. Piccolella, M. Gilliet, L. Frasca, The antimicrobial peptide LL37 is a T-cell autoantigen in psoriasis. *Nat. Commun.* 5, 5621 (2014).
- A. Arakawa, K. Siewert, J. Stohr, P. Besgen, S. M. Kim, G. Ruhl, J. Nickel, S. Vollmer, P. Thomas, S. Krebs, S. Pinkert, M. Spannagl, K. Held, C. Kammerbauer, R. Besch, K. Dornmair, J. C. Prinz, Melanocyte antigen triggers autoimmunity in human psoriasis. J. Exp. Med. 212, 2203–2212 (2015).
- S. Nishimoto, H. Kotani, S. Tsuruta, N. Shimizu, M. Ito, T. Shichita, R. Morita, H. Takahashi, M. Amagai, A. Yoshimura, Th17 cells carrying TCR recognizing epidermal autoantigen induce psoriasis-like skin inflammation. *J. Immunol.* 191, 3065–3072 (2013).
- O. J. Iversen, H. Lysvand, G. Slupphaug, Pso p27, a SERPINB3/B4-derived protein, is most likely a common autoantigen in chronic inflammatory diseases. *Clin. Immunol.* 174, 10–17 (2017).
- K. L. Cheung, R. Jarrett, S. Subramaniam, M. Salimi, D. Gutowska-Owsiak, Y. L. Chen, C. Hardman, L. Xue, V. Cerundolo, G. Ogg, Psoriatic T cells recognize neolipid antigens generated by mast cell phospholipase delivered by exosomes and presented by CD1a. J. Exp. Med. 213, 2399–2412 (2016).
- O. Rotzschke, K. Falk, H. J. Wallny, S. Faath, H. G. Rammensee, Characterization of naturally occurring minor histocompatibility peptides including H-4 and H-Y. Science 249, 283–287 (1990).
- J. G. Abelin, E. J. Bergstrom, K. D. Rivera, H. B. Taylor, S. Klaeger, C. Xu, E. K. Verzani,
 C. Jackson White, H. B. Woldemichael, M. Virshup, M. E. Olive, M. Maynard, S. A. Vartany,
 J. D. Allen, K. Phulphagar, M. Harry Kane, S. Rachimi, D. R. Mani, M. A. Gillette, S. Satpathy,
 K. R. Clauser, N. D. Udeshi, S. A. Carr, Workflow enabling deepscale immunopeptidome,
 proteome, ubiquitylome, phosphoproteome, and acetylome analyses of sample-limited
 tissues. Nat. Commun. 14, 1851 (2023).
- L. K. Freudenmann, A. Marcu, S. Stevanovic, Mapping the tumour human leukocyte antigen (HLA) ligandome by mass spectrometry. *Immunology* 154, 331–345 (2018).
- A. M. Jaeger, L. E. Stopfer, R. Ahn, E. A. Sanders, D. A. Sandel, W. A. Freed-Pastor, W. M. Rideout III, S. Naranjo, T. Fessenden, K. B. Nguyen, P. S. Winter, R. E. Kohn, P. M. K. Westcott, J. M. Schenkel, S. L. Shanahan, A. K. Shalek, S. Spranger, F. M. White, T. Jacks, Deciphering the immunopeptidome in vivo reveals new tumour antigens. Nature 607, 149–155 (2022).
- Y. Sun, N. Sheshadri, W. X. Zong, SERPINB3 and B4: From biochemistry to biology. Semin. Cell Dev. Biol. 62, 170–177 (2017).
- U. Sivaprasad, D. J. Askew, M. B. Ericksen, A. M. Gibson, M. T. Stier, E. B. Brandt, S. A. Bass, M. O. Daines, J. Chakir, K. F. Stringer, S. E. Wert, J. A. Whitsett, T. D. Le Cras, M. Wills-Karp, G. A. Silverman, G. K. Khurana Hershey, A nonredundant role for mouse Serpinb3a in the induction of mucus production in asthma. J. Allergy Clin. Immunol. 127, 254–261.e6 (2011).
- R. M. Chicz, R. G. Urban, J. C. Gorga, D. A. Vignali, W. S. Lane, J. L. Strominger, Specificity and promiscuity among naturally processed peptides bound to HLA-DR alleles. *J. Exp. Med.* 178, 27–47 (1993).
- O. Rotzschke, K. Falk, Origin, structure and motifs of naturally processed MHC class II ligands. Curr. Opin. Immunol. 6, 45–51 (1994).
- F. Sinigaglia, J. Hammer, Defining rules for the peptide-MHC class II interaction. Curr. Opin. Immunol. 6, 52–56 (1994).
- S. Costa, D. Bevilacqua, E. Caveggion, S. Gasperini, E. Zenaro, F. Pettinella, M. Donini,
 Dusi, G. Constantin, S. Lonardi, W. Vermi, F. De Sanctis, S. Ugel, T. Cestari, C. L. Abram,
 A. Lowell, P. Rodegher, F. Tagliaro, G. Girolomoni, M. A. Cassatella, P. Scapini,
 Neutrophils inhibit gammadelta T cell functions in the imiquimod-induced mouse model of psoriasis. Front. Immunol. 13, 1049079 (2022).
- F. Li, D. Han, B. Wang, W. Zhang, Y. Zhao, J. Xu, L. Meng, K. Mou, S. Lu, W. Zhu, Y. Zhou,
 Topical treatment of colquhounia root relieves skin inflammation and itch in
 imiquimod-induced psoriasiform dermatitis in mice. *Mediators Inflamm.* 2022, 5782922
 (2022).
- L. van der Fits, S. Mourits, J. S. Voerman, M. Kant, L. Boon, J. D. Laman, F. Cornelissen, A. M. Mus, E. Florencia, E. P. Prens, E. Lubberts, Imiquimod-induced psoriasis-like skin inflammation in mice is mediated via the IL-23/IL-17 axis. *J. Immunol.* 182, 5836–5845 (2009).
- F. Lauffer, K. Eyerich, Eczematized psoriasis—A frequent but often neglected variant of plaque psoriasis. J. Dtsch. Dermatol. Ges. 21, 445–453 (2023).
- H. Vinter, L. Iversen, T. Steiniche, K. Kragballe, C. Johansen, Aldara(R)-induced skin inflammation: Studies of patients with psoriasis. Br. J. Dermatol. 172, 345–353 (2015).
- N. Garzorz-Stark, F. Lauffer, L. Krause, J. Thomas, A. Atenhan, R. Franz, S. Roenneberg,
 A. Boehner, M. Jargosch, R. Batra, N. S. Mueller, S. Haak, C. Gross, O. Gross,
 C. Traidl-Hoffmann, F. J. Theis, C. B. Schmidt-Weber, T. Biedermann, S. Eyerich, K. Eyerich,

SCIENCE ADVANCES | RESEARCH ARTICLE

- Toll-like receptor 7/8 agonists stimulate plasmacytoid dendritic cells to initiate TH17-deviated acute contact dermatitis in human subjects. *J. Allergy Clin. Immunol.* **141**, 1320–1333.e11 (2018).
- A. Al-Janabi, A. C. Foulkes, C. E. M. Griffiths, R. B. Warren, Paradoxical eczema in patients with psoriasis receiving biologics: A case series. Clin. Exp. Dermatol. 47, 1174–1178 (2022).
- Y. Zhang, G. Jiang, Application of JAK inhibitors in paradoxical reaction through immune-related dermatoses. Front. Immunol. 15, 1341632 (2024).
- N. Garzorz-Stark, L. Krause, F. Lauffer, A. Atenhan, J. Thomas, S. P. Stark, R. Franz,
 S. Weidinger, A. Balato, N. S. Mueller, F. J. Theis, J. Ring, C. B. Schmidt-Weber,
 T. Biedermann, S. Eyerich, K. Eyerich, A novel molecular disease classifier for psoriasis and eczema. *Exp. Dermatol.* 25, 767–774 (2016).
- M. Bassani-Sternberg, E. Braunlein, R. Klar, T. Engleitner, P. Sinitcyn, S. Audehm, M. Straub, J. Weber, J. Slotta-Huspenina, K. Specht, M. E. Martignoni, A. Werner, R. Hein, D. H. Busch, C. Peschel, R. Rad, J. Cox, M. Mann, A. M. Krackhardt, Direct identification of clinically relevant neoepitopes presented on native human melanoma tissue by mass spectrometry. *Nat. Commun.* 7, 13404 (2016).
- A. Marcu, L. Bichmann, L. Kuchenbecker, D. J. Kowalewski, L. K. Freudenmann, L. Backert, L. Muhlenbruch, A. Szolek, M. Lubke, P. Wagner, T. Engler, S. Matovina, J. Wang, M. Hauri-Hohl, R. Martin, K. Kapolou, J. S. Walz, J. Velz, H. Moch, L. Regli, M. Silginer, M. Weller, M. W. Loffler, F. Erhard, A. Schlosser, O. Kohlbacher, S. Stevanovic, H. G. Rammensee, M. C. Neidert, HLA ligand atlas: A benign reference of HLA-presented peptides to improve T-cell-based cancer immunotherapy. J. Immunother. Cancer 9, eabn9644 (2021).
- C. R. Parish, Cancer immunotherapy: The past, the present and the future. *Immunol. Cell Biol.* 81, 106–113 (2003).
- V. Velcheti, K. Schalper, Basic overview of current immunotherapy approaches in cancer. Am. Soc. Clin. Oncol. Educ. Book 35, 298–308 (2016).
- M. Y. Mapara, M. Sykes, Tolerance and cancer: Mechanisms of tumor evasion and strategies for breaking tolerance. J. Clin. Oncol. 22, 1136–1151 (2004).
- D. Mougiakakos, G. Kronke, S. Volkl, S. Kretschmann, M. Aigner, S. Kharboutli, S. Boltz, B. Manger, A. Mackensen, G. Schett, CD19-targeted CART cells in refractory systemic lupus erythematosus. N. Engl. J. Med. 385, 567–569 (2021).
- C. Krienke, L. Kolb, E. Diken, M. Streuber, S. Kirchhoff, T. Bukur, O. Akilli-Ozturk, L. M. Kranz, H. Berger, J. Petschenka, M. Diken, S. Kreiter, N. Yogev, A. Waisman, K. Kariko, O. Tureci, U. Sahin, A noninflammatory mRNA vaccine for treatment of experimental autoimmune encephalomyelitis. *Science* 371, 145–153 (2021).
- J. G. Krueger, An autoimmune "attack" on melanocytes triggers psoriasis and cellular hyperplasia. J. Exp. Med. 212, 2186 (2015).
- A. Takeda, D. Higuchi, T. Takahashi, M. Ogo, P. Baciu, P. F. Goetinck, T. Hibino, Overexpression of serpin squamous cell carcinoma antigens in psoriatic skin. J. Invest. Dermatol. 118, 147–154 (2002).
- J. Fuentes-Duculan, K. M. Bonifacio, J. E. Hawkes, N. Kunjravia, I. Cueto, X. Li, J. Gonzalez, S. Garcet, J. G. Krueger, Autoantigens ADAMTSL5 and LL37 are significantly upregulated in active psoriasis and localized with keratinocytes, dendritic cells and other leukocytes. Exp. Dermatol. 26, 1075–1082 (2017).
- M. Bassani-Sternberg, S. Pletscher-Frankild, L. J. Jensen, M. Mann, Mass spectrometry of human leukocyte antigen class I peptidomes reveals strong effects of protein abundance and turnover on antigen presentation. *Mol. Cell. Proteomics* 14, 658–673 (2015).
- F. Numa, O. Takeda, M. Nakata, S. Nawata, N. Tsunaga, K. Hirabayashi, Y. Suminami, H. Kato, S. Hamanaka, Tumor necrosis factor-alpha stimulates the production of squamous cell carcinoma antigen in normal squamous cells. *Tumour Biol.* 17, 97–101 (1996).
- Y. Uemura, S. C. Pak, C. Luke, S. Cataltepe, C. Tsu, C. Schick, Y. Kamachi, S. L. Pomeroy,
 D. H. Perlmutter, G. A. Silverman, Circulating serpin tumor markers SCCA1 and SCCA2 are not actively secreted but reside in the cytosol of squamous carcinoma cells. *Int. J. Cancer* 89, 368–377 (2000).
- A. Schabitz, C. Hillig, M. Mubarak, M. Jargosch, A. Farnoud, E. Scala, N. Kurzen, A. C. Pilz, N. Bhalla, J. Thomas, M. Stahle, T. Biedermann, C. B. Schmidt-Weber, F. Theis, N. Garzorz-Stark, K. Eyerich, M. P. Menden, S. Eyerich, Spatial transcriptomics landscape of lesions from non-communicable inflammatory skin diseases. *Nat. Commun.* 13, 7729 (2022).
- H. Maciejewska-Rodrigues, M. Al-Shamisi, H. Hemmatazad, C. Ospelt, M. C. Bouton,
 D. Jager, A. P. Cope, P. Charles, D. Plant, J. H. Distler, R. E. Gay, B. A. Michel, A. Knuth,
 M. Neidhart, S. Gay, A. Jungel, Functional autoantibodies against serpin E2 in rheumatoid arthritis. Arthritis Rheum. 62, 93–104 (2010).
- Y. Kryvalap, M. L. Jiang, N. Kryvalap, C. Hendrickson, J. Czyzyk, SerpinB13 antibodies promote β cell development and resistance to type 1 diabetes. Sci. Transl. Med. 13, eabf1587 (2021).
- M. Gatto, L. Iaccarino, A. Ghirardello, N. Bassi, P. Pontisso, L. Punzi, Y. Shoenfeld, A. Doria, Serpins, immunity and autoimmunity: Old molecules, new functions. Clin Rev Allergy Immunol 45, 267–280 (2013).

- H. Lysvand, R. Helland, L. Hagen, G. Slupphaug, O. J. Iversen, Psoriasis pathogenesis—Pso p27 constitutes a compact structure forming large aggregates. *Biochem. Biophys. Rep.* 2, 132–136 (2015).
- H. Lysvand, L. Hagen, L. Klubicka, G. Slupphaug, O. J. Iversen, Psoriasis pathogenesis—Pso p27 is generated from SCCA1 with chymase. *Biochim. Biophys. Acta* 1842, 734–738 (2014).
- 57. Y. Nagata, R. Suzuki, FcepsilonRl: A master regulator of mast cell functions. *Cells* 11, 622 (2022)
- K. Mukai, M. Tsai, H. Saito, S. J. Galli, Mast cells as sources of cytokines, chemokines, and growth factors. *Immunol. Rev.* 282, 121–150 (2018).
- D. Simon, E. Vassina, S. Yousefi, E. Kozlowski, L. R. Braathen, H. U. Simon, Reduced dermal infiltration of cytokine-expressing inflammatory cells in atopic dermatitis after short-term topical tacrolimus treatment. J. Allergy Clin. Immunol. 114, 887–895 (2004).
- W. Xiao, K. Sha, M. Wang, Z. Tan, Y. Wang, S. Xu, Z. Zhao, Q. Wang, H. Xie, M. Chen, Z. Deng, J. Li, SERPINB3/B4 is increased in psoriasis and rosacea lesions and has proinflammatory effects in mouse models of these diseases. *J. Invest. Dermatol.* 144, 2706–2718.e6 (2024).
- T. R. Matos, J. T. O'Malley, E. L. Lowry, D. Hamm, I. R. Kirsch, H. S. Robins, T. S. Kupper, J. G. Krueger, R. A. Clark, Clinically resolved psoriatic lesions contain psoriasis-specific IL-17-producing alphabeta T cell clones. *J. Clin. Invest.* 127, 4031–4041 (2017).
- S. M. Lwin, J. A. Snowden, C. E. M. Griffiths, The promise and challenges of cell therapy for psoriasis. Br. J. Dermatol. 185, 887–898 (2021).
- 63. K. Schakel, K. Reich, K. Asadullah, A. Pinter, D. Jullien, P. Weisenseel, C. Paul, M. Gomez, S. Wegner, Y. Personke, F. Kreimendahl, Y. Chen, J. Angsana, M. W. L. Leung, K. Eyerich, Early disease intervention with guselkumab in psoriasis leads to a higher rate of stable complete skin clearance ('clinical super response'): Week 28 results from the ongoing phase IIIb randomized, double-blind, parallel-group, GUIDE study.

 J. Eur. Acad. Dermatol. Venerool. 37, 2016–2027 (2023).
- L. Iversen, C. Conrad, L. Eidsmo, A. Costanzo, J. Narbutt, A. Pinter, K. Kingo, R. Rivera Diaz, F. Kolbinger, M. Nanna, J. A. Frueh, P. Jagiello, Secukinumab demonstrates superiority over narrow-band ultraviolet B phototherapy in new-onset moderate to severe plaque psoriasis patients: Week 52 results from the STEPIn study. J. Eur. Acad. Dermatol. Venereol. 37, 1004–1016 (2023).
- D. J. Kowalewski, S. Stevanovic, Biochemical large-scale identification of MHC class I liqands. Methods Mol. Biol. 960, 145–157 (2013).
- C. J. Barnstable, W. F. Bodmer, G. Brown, G. Galfre, C. Milstein, A. F. Williams, A. Ziegler, Production of monoclonal antibodies to group A erythrocytes, HLA and other human cell surface antigens-new tools for genetic analysis. *Cell* 14, 9–20 (1978).
- G. Pawelec, A. Ziegler, P. Wernet, Dissection of human allostimulatory determinants with cloned T cells: Stimulation inhibition by monoclonal antibodies TU22, 34, 35, 36, 37, 39, 43, and 58 against distinct human MHC class II molecules. *Hum. Immunol.* 12, 165–176 (1985).
- J. M. Goldman, J. Hibbin, L. Kearney, K. Orchard, K. H. Th'ng, HLA-DR monoclonal antibodies inhibit the proliferation of normal and chronic granulocytic leukaemia myeloid progenitor cells. Br. J. Haematol. 52, 411–420 (1982).
- D. J. Kowalewski, H. Schuster, L. Backert, C. Berlin, S. Kahn, L. Kanz, H. R. Salih, H. G. Rammensee, S. Stevanovic, J. S. Stickel, HLA ligandome analysis identifies the underlying specificities of spontaneous antileukemia immune responses in chronic lymphocytic leukemia (CLL). *Proc. Natl. Acad. Sci. U.S.A.* 112, E166–E175 (2015).
- J. K. Eng, A. L. McCormack, J. R. Yates, An approach to correlate tandem mass spectral data of peptides with amino acid sequences in a protein database.
 J. Am. Soc. Mass Spectrom. 5, 976–989 (1994).
- P. Speth, M. Jargosch, P. Seiringer, K. Schwamborn, T. Bauer, C. Scheerer, U. Protzer, C. Schmidt-Weber, T. Biedermann, S. Eyerich, N. Garzorz-Stark, Immunocompromised patients with therapy-refractory chronic skin diseases show reactivation of latent Epstein–Barr virus and cytomegalovirus infection. *J. Invest. Dermatol.* 142, 549–558.e6 (2022).
- F. Lauffer, M. Jargosch, L. Krause, N. Garzorz-Stark, R. Franz, S. Roenneberg, A. Bohner, N. S. Mueller, F. J. Theis, C. B. Schmidt-Weber, T. Biedermann, S. Eyerich, K. Eyerich, Type I immune response induces keratinocyte necroptosis and is associated with interface dermatitis. J. Invest. Dermatol. 138, 1785–1794 (2018).
- Z. Kurgyis, L. Vornholz, K. Pechloff, L. V. Kemeny, T. Wartewig, A. Muschaweckh, A. Joshi, K. Kranen, L. Hartjes, S. Mockel, K. Steiger, E. Hameister, T. Volz, M. Mellett, L. E. French, T. Biedermann, T. Korn, J. Ruland, Keratinocyte-intrinsic BCL10/MALT1 activity initiates and amplifies psoriasiform skin inflammation. Sci. Immunol. 6, eabi4425 (2021).
- T. Sparwasser, R. M. Vabulas, B. Villmow, G. B. Lipford, H. Wagner, Bacterial CpG-DNA activates dendritic cells in vivo: T helper cell-independent cytotoxic T cell responses to soluble proteins. Eur. J. Immunol. 30, 3591–3597 (2000).
- A. Lemieux, G. Sannier, A. Nicolas, M. Nayrac, G. G. Delgado, R. Cloutier, N. Brassard, M. Laporte, M. Duchesne, A. M. Sreng Flores, A. Finzi, O. Tastet, M. Dube, D. E. Kaufmann, Enhanced detection of antigen-specific T cells by a multiplexed AIM assay. *Cell Rep. Methods* 4, 100690 (2024).

SCIENCE ADVANCES | RESEARCH ARTICLE

- S. Lavazais, M. Jargosch, S. Dupont, F. Labeguere, C. Menet, C. Jagerschmidt, F. Ohm, L. Kupcsik, I. Parent, C. Cottereaux, F. Marsais, L. Oste, A. Van de Water, T. Christophe, S. De Vos, P. Fallon, F. Lauffer, P. Clement-Lacroix, K. Eyerich, R. Brys, IRAK4 inhibition dampens pathogenic processes driving inflammatory skin diseases. Sci. Transl. Med. 15, eabj3289 (2023).
- A. Bohner, M. Jargosch, N. S. Muller, N. Garzorz-Stark, C. Pilz, F. Lauffer, R. Wang, S. Roenneberg, A. Zink, J. Thomas, F. J. Theis, T. Biedermann, S. Eyerich, K. Eyerich, The neglected twin: Nummular eczema is a variant of atopic dermatitis with co-dominant T_H2/T_H17 immune response. *J. Allergy Clin. Immunol.* 152, 408–419
- M. I. Love, W. Huber, S. Anders, Moderated estimation of fold change and dispersion for RNA-seq data with DESeq2. Genome Biol. 15, 550 (2014).
- P. Bankhead, M. B. Loughrey, J. A. Fernandez, Y. Dombrowski, D. G. McArt, P. D. Dunne, S. McQuaid, R. T. Gray, L. J. Murray, H. G. Coleman, J. A. James, M. Salto-Tellez, P. W. Hamilton, QuPath: Open source software for digital pathology image analysis. Sci. Rep. 7, 16878 (2017).

Acknowledgments: We thank K. Weber, J. Sänger, D. Arigiu, C. Knappe, N. Bauer, C. Falkenburger, P. Hrstić, B. Pömmerl, and U. Wulle for excellent technical support; V. Baghin for the active assistance with patient recruitment; and R. Batra for assistance with bioinformatic analysis. We would also like to thank the editors for their editorial support. Funding: This work was funded by the German Research Foundation (DFG): (i) GRK2668 "Immune Master Switches in Allergies and Autoimmune Diseases" (Projects A1, A2, and B3, Project ID: 435874434) (T.B., S.E., C.B.S.-W., N.G.-S., F.L., J.K., Y.K., and J.E.) and (ii) Project ID 434262558 (N.G.-S.) and GSC 81

"International Graduate School of Science and Engineering (IGSSE) (M.P.M. and C.H.). Author contributions: Conceptualization: M.J., C.B.S.-W., J.S.W., T.B., H.-G.R., S.E., K.E., Z.K., L.K.F., and N.G.-S. Methodology: M.J., J.K., D.J.K., J.S.W., E.S., S.B., J.G., A.B., J.T., H.-G.R., L.K.F., C.H., T.B., S.E., Z.K., and N.G.-S. Investigation: M.J., J.K., J.E., S.B., J.S.W., S.L., D.J.K., S.W., Y.K., E.S., J.G., C.H., Z.K., L.K.F., A.B., and N.G.-S. Validation: M.J., S.L., E.S., N.T., J.S.W., T.B., K.E., Z.K., L.K.F., and N.G.-S. Visualization: C.H., M.J., L.K.F., and Z.K. Funding acquisition: T.B., J.S.W., H.-G.R., S.E., K.E., Z.K., and N.G.-S. Supervision: M.J., C.B.S.-W., D.J.K., H.-G.R., T.B., S.E., K.E., Z.K., and N.G.-S. Writing original draft: M.J., N.G.-S., C.B.S.-W., and L.K.F. Writing—review and editing: M.J., E.S., D.J.K., C.H., J.T., J.G., C.B.S.-W., M.P.M., J.S.W., S.K., S.E., S.B., F.L., T.B., K.E., Z.K., L.K.F., and N.G.-S. Data curation: J.S.W., M.J., C.H., K.E., L.K.F., and N.G.-S. Formal analysis: M.J., N.T., C.H., J.S.W., Z.K., L.K.F., and N.G.-S. Resources: A.B., S.B., C.B.S.-W., J.S.W., S.K., J.G., H.-G.R., T.B., S.E., K.E., Z.K., and N.G.-S. Project administration: M.J., T.B., C.B.S.-W., L.K.F., and N.G.-S. Competing interests: The authors declare that they have no competing interests. Data and materials availability: Bulk RNA-seg data related to this article can be obtained at GEO (www.ncbi.nlm.nih.gov/) under the accession number GSE154200 (https://ncbi.nlm.nih.gov/geo/query/acc.cgi?acc=GSE154200). Spatial RNA-seq data can be obtained at GEO (www.ncbi.nlm.nih.gov) under the accession number: GSE206391 (https://ncbi.nlm.nih.gov/geo/query/acc.cgi?acc=GSE206391). All data needed to evaluate the conclusions in the paper are present in the paper and/or the Supplementary Materials.

Submitted 26 February 2025 Accepted 25 September 2025 Published 22 October 2025 10.1126/sciadv.adx0637